

N79-24298
final report
CR-152267

(NASA-CR-152267) DESIGN, FABRICATION AND
TEST OF A HYDROGEN HEAT PIPE Final Report
(Grumman Aerospace Corp.) 76 p.
HC-A05/MF A01

N79-24298

CSCL 20D

Unclass

G3/34 21101

DESIGN, FABRICATION AND TEST OF A HYDROGEN HEAT PIPE



GRUMMAN AEROSPACE CORPORATION

DESIGN, FABRICATION AND TEST
OF A
HYDROGEN HEAT PIPE

FINAL REPORT

Prepared for

NASA/AMES RESEARCH CENTER
MOFFETT FIELD, CALIFORNIA 94035
CONTRACT NAS2-9291
by
GRUMMAN AEROSPACE CORPORATION
BETHHPAGE, NEW YORK 11714

Prepared by: J. Alario

Approved by: R. Haslett

February 1979

FOREWORD

This report was prepared by Grumman Aerospace Corporation for the Ames Research Center of the National Aeronautics and Space Administration. The work was done under Contract NAS 2-9291, from August 1976 to February 1979. Dr. C. McCreight was the NASA technical monitor. Grumman personnel were Mr. R. Haslett, Program Manager, and Mr. J. Alario, Project Engineer.

Foremost, we wish to acknowledge the guidance, patience and understanding given by Dr. C. McCreight in this ambitious extension of heat pipe technology. Many unanticipated difficulties were encountered before finally obtaining an acceptable re-entrant groove extrusion. However, the experience and knowledge gained in this program represent a significant forward step in developing improved heat pipe hardware. Many fundamental contributions were made by Dr. R. Kosson who was responsible for the optimization analysis and for wise counsel whenever called upon. Finally, Mr. R. Carey of the Micro Extrusions Division, Universal Alloy Corp., is acknowledged for his interest and dogged persistence in pushing the state-of-the art in extrusion technology.

CONTENTS

<u>Section</u>		<u>Page</u>
	FOREWORD	iii
1	SUMMARY	1-1
2	INTRODUCTION	2-1
3	CANDIDATE HEAT PIPE DESIGNS	3-1
4	PARAMETRIC STUDY OF RE-ENTRANT GROOVE GEOMETRIES	4-1
5	DESCRIPTION OF THE RE-ENTRANT GROOVE EXTRUSION	5-1
5.1	The Extrusion	5-1
5.2	Theoretical Performance	5-2
5.3	Storage Pressure Containment	5-5
6	HEAT PIPE DESIGN AND FABRICATION	6-1
6.1	Charge Requirement	6-1
6.2	Charge Procedure	6-4
6.3	Strength Check	6-5
6.3.1	Heat Pipe	6-5
6.3.2	Reservoir	6-5
7	TEST EVALUATION	7-1
7.1	Instrumentation	7-1
7.2	Tests with Ammonia	7-2
7.2.1	Test Setup	7-2
7.2.2	Results	7-4
7.3	Tests with Hydrogen	7-7
7.3.1	Test Setup	7-7
7.3.2	Hydrogen Test Results	7-15
8	IMPROVED RE-ENTRANT GROOVE CONFIGURATION	8-1
9	CONCLUSIONS	9-1
10	REFERENCES	10-1

CONTENTS (Cont)

<u>Section</u>	<u>Page</u>
APPENDIX A - COMPUTER CODE FOR PARAMETRIC STUDY OF RE-ENTRANT GROOVE GEOMETRIES	A-1
APPENDIX B - SAFE HANDLING AND STORAGE PROCEDURES FOR HYDROGEN HEAT PIPES	B-1
APPENDIX C - SAFE HANDLING AND STORAGE OF LIQUID HELIUM	C-1

ILLUSTRATIONS

<u>Fig.</u>		<u>Page</u>
1	Diffusion of Hydrogen Through Metals	3-2
2	Performance Comparison of Candidate Wicking Systems (Hydrogen @ 20 K)	3-3
3	Pressure Containment vs Volume Ratio	3-3
4	Re-Entrant Groove Geometry Used for Parametrics	4-1
5	Transport Capacity and Reservoir Volume vs Number of Grooves for Constant Wall Thickness	4-4
6	Transport Capacity and Reservoir Volume vs Number of Grooves for Constant Groove Diameter	4-4
7	Effect of Increasing Outside Diameter, Keeping Inside Geometry Constant	4-6
8	Transport Capacity vs Number of Grooves with Wall Thickness Adequate to Eliminate Reservoir	4-6
9	Specified Design Geometry	5-3
10	Photomicrograph of Re-Entrant Groove Extrusion	5-3
11	Manufacturing Plan for Hydrogen Heat Pipe	6-2
12	Hydrogen Heat Pipe Final Assembly, on Test Stand	6-3
13	Charging Set-Up/Procedure for Hydrogen HP	6-6
14	Heat Pipe Test Instrumentation	7-3
15	Low Temperature Thermocouple Schematic	7-3
16	Performance of NASA-AMES Re-Entrant Groove Heat Pipe with Ammonia @ 20°C	7-5
17	Re-Entrant Groove Extrusion with Ammonia, Temperature Gradients	7-6
18	Low Temperature T/V Chamber Test Set-Up - End View	7-8
19	Flow Schematic - Low Temperature Facility	7-10
20	Heat Pipe Assembly Standoff Supports (Mat'l Teflon)	7-14
21	Cool Down Transient	7-16
22	Hydrogen Heat Pipe Performance Data, Q_{MAX} vs HP Tilt	7-18
23	Hydrogen HP Performance, Overall Temperature Gradient	7-19
24	Hydrogen HP Performance, Temperature Profiles	7-20

ILLUSTRATIONS (Cont)

<u>Fig.</u>		<u>Page</u>
25	Heat Pipe Recovery from Frozen Condition	7-21
26	Improved Re-Entrant Groove HP Performance	8-2

TABLES

<u>Table</u>		<u>Page</u>
1	Characteristic Dimensions of the Hydrogen Heat Pipe Extrusion	5-4
2	Burst Pressure Test Results for 6063 Aluminum Axially Grooved Extrusions	5-5

Section 1

SUMMARY

This program extends the development of re-entrant groove technology to hydrogen heat pipes. Parametric analyses are presented which optimize the theoretical design while considering the limitations of state-of-the art extrusion technology. Acceptable production-type runs of extruded lengths (over 100 meters) could only be achieved at the expense of a wider nominal groove opening than specified (0.33 mm vs 0.20 mm). However, dimensional variations of other critical dimensions were within 0.05 mm, which exceeded expectations. The 6063-T6 aluminum extrusion is 14.6 mm OD with a wall thickness of 1.66 mm and contains 20 axial grooves which surround a central 9.3 mm diameter vapor core. Each axial groove is 0.775 mm diameter with a 0.33 mm opening. An excess vapor reservoir is provided at the evaporator to minimize the pressure containment hazard during ambient storage.

Tests were first conducted with ammonia (at room temperature) to accurately determine the proper working fluid charge for the 100 cm long heat pipe. The data indicated that 8 grams of ammonia at 20°C was the 100 percent charge value. The corresponding vapor and liquid areas for the heat pipe only were found to be 0.697 cm^2 and 0.1302 cm^2 , respectively. The hydrogen charge requirement (with a 5 percent overcharge, including reservoir) was calculated to be 1.2 grams at the 20 K operating point.

Test results with ammonia were lower than predictions using the nominal geometry measurements. At 100 percent charge the maximum transport capacity was 110 w-m and the static wicking height was 1.65 cm, which was 19 percent and 22 percent lower than the respective predicted values. The corresponding film heat transfer coefficients measured were $2014 \text{ w/m}^{20} \text{ C}$ for the evaporator and $5362 \text{ w/m}^{20} \text{ C}$ for the condenser, for an equivalent overall heat pipe conductance of 5.85 watts/ $^{\circ}\text{C}$.

Modifications to the basic re-entrant groove profile, which were accomplished under an independent company effort, resulted in improved overall performance. While the maximum heat transport capacity decreased slightly to 103 w-m the static wicking height increased markedly to 4.5 cm. More importantly, the evaporator and condenser film coefficients improved to $7900 \text{ w/m}^{20} \text{ C}$ and $14000 \text{ w/m}^{20} \text{ C}$, respectively. The overall heat pipe conductance increased almost 400 percent to 20.2 watts/ $^{\circ}\text{C}$.

The hydrogen test program went very smoothly and all objectives were achieved. The heat pipe became operational between 20 and 30 K after a cooldown from 77 K without any difficulty. Steady state performance data taken over a 19 to 23 K temperature range indicated the following:

- Maximum heat transport capacity = 5.4 w-m
- Static wicking height = 1.42 cm
- Overall heat pipe conductance = 1.7 watts/°C.

These data agree remarkably well with extrapolations made from the ammonia test results. The maximum heat transport capacity is 9.5% larger than the extrapolated value, but the static wicking height is the same. The overall conductance is 29 percent of the ammonia value, which is close to the ratio of liquid thermal conductivities (24 percent).

Recovery from a completely frozen condition was accomplished within five minutes by simply applying an evaporator heat load of 1.8 watts.

Section 2

INTRODUCTION

Cryogenic technology is advancing rapidly in both space and earth-based applications, and with it comes the need for near-liquid helium-temperature thermal control systems. The hydrogen heat pipe is a device that can be successfully applied to many potential areas that have recently been identified for this temperature regime.

Sensitive infrared detectors such as doped-silicon photoconductors operate at or below temperatures in the range of 15-25 K. Components of orbiting infrared telescopes, such as telescope barrels, mirrors, choppers, and baffles, will require cryogenic cooling and iso-thermalization to reduce telescope thermal emission. Also in support of fusion reactor technology, super-conducting magnets must be cooled below their transition temperature. A hydrogen heat pipe could provide an efficient thermal coupling to stored cryogens, such as solid hydrogen or liquid helium, or to cryogenic refrigerators, while also permitting the design flexibility of separate locations for the cooler and the component being cooled.

What has become known as the "standard" axially grooved aluminum extrusion was developed by NASA-GSFC as part of the ATS-F satellite program in order to provide heat pipes with cleaner, more dimensionally uniform grooving than that previously obtainable with a swage-forging process. The extruded tubing was successfully produced by Micro Extrusions Division of Universal Alloy Corp., Anaheim, CA, in production quantities. It contains 27 axial grooves, each one with a nearly rectangular profile, 0.66 mm wide by 1.02 mm deep. Since its development, it has been used to make heat pipes for cryogenic (>100 K) to moderate temperatures using working fluids such as methane, ethane, Freon-21 and ammonia^{1,2,3}. Although the NASA-GSFC extrusion is an improvement over the original swaged tubing, providing reasonable heat transport capacity with a wide range of working fluids, it has very poor tilt capability. This presents difficulties in obtaining reliable ground test data at anything but low heat loads.

In an effort to make axially grooved heat pipes less tilt sensitive, NASA-Lewis Research Center (LeRC) developed a re-entrant groove profile which promised comparable heat transport capacity but much better static wicking height than the rectangular grooves. The NASA-LeRC design was also produced by Micro Extrusions, but only about 3 meters could be extruded before the die broke. Under contract to NASA-LeRC, the Grumman Aerospace Corporation analyzed, built, and tested a heat pipe made from this re-entrant groove tubing⁴.

The extrusion had a 13 mm diameter with a 0.64 mm wall thickness, and contained 20 axial grooves. Each groove had a "key hole" profile with a nominal 0.8 mm diameter liquid flow channel and a 0.2 mm wide slightly tapered passageway which connected the channel to a 9.28 mm diameter vapor core. The dimensional uniformity of the extrusion was good and test results with ammonia working fluid were excellent. When compared to the standard rectangular groove extrusion, the re-entrant groove had double the static wicking height (25.1 mm vs 12.0 mm) and a 12% higher zero-g heat transport capacity (143 W-m vs 127 W-m). The overall heat transfer film coefficient, however, was about 20% lower (5380 W/m²°C vs 6860 W/m²°C), being higher in the condenser due to increased groove land area, and lower in the evaporator due primarily to the fewer grooves.

Overall, the re-entrant groove profile demonstrated a definite improvement in axially grooved heat pipes, thus increasing performance while maintaining simplicity. For cryogenic applications, the re-entrant groove has the additional advantage of requiring less charge. Since these characteristics had definite advantages when applied to the cryogenic heat pipe fluids, NASA-Ames Research Center (ARC), under contract with Grumman, proceeded to develop a re-entrant groove extrusion that was suitable for use with hydrogen and which could also be produced in meaningful quantity. Performance objectives for a one meter long heat pipe operating at a temperature of 20 K call for an equivalent zero-g heat transport capacity of 8 watt-meters, and a 4 watt-meter capacity at 5 mm adverse tilt.

The following sections present the development of the first re-entrant groove hydrogen heat pipe by describing the design parametrics, detailing the characteristics of the heat pipe extrusion and describing the test evaluation using both ammonia and hydrogen working fluids.

Section 3

CANDIDATE HEAT PIPE DESIGNS

A basic design problem concerns the choice of materials for the tube envelope and reservoir which minimize the potential for hydrogen embrittlement and subsequent material failure. The hydrogen embrittlement phenomenon peaks around room temperature and is thought to be related to the corresponding diffusion rates. Of the materials commonly used for heat pipes, aluminum is far less susceptible to hydrogen diffusion and the associated embrittlement effects. As shown in Figure 1, when compared to the high strength steels, the diffusion rates in aluminum are seven orders of magnitude less. In addition, the axial groove profiles desired for the simple cryogenic heat pipes are more readily obtained in extruded aluminum tubes than forged steel tubing. Thus, considering both potential embrittlement problems and producibility, aluminum was selected as the heat pipe material.

The choice of a wicking system is primarily a trade-off between performance and containment pressure considerations. A theoretical performance comparison of candidate wicking systems (axial groove, slab wick, spiral artery) in a nominal 12.7 mm diameter tube is given in Figure 2 for hydrogen at 20 K. Generalized pressure containment data is presented in Figure 3 as a function of heat pipe vapor/liquid volume ratio for a 322 K maximum storage temperature. Pressures were calculated using the virial form of the equation of state as given in Reference 5.

$$P = RT \bar{\rho} \left[1 + B(T) \bar{\rho} + C(T) \bar{\rho}^2 \right]$$

where $R = 0.08206 \text{ atm} \cdot \text{m}^3/\text{g-mol K}$, $T = \text{temperature (K)}$, $\bar{\rho} = \text{density (mol/cc)}$ and $B(T)$ and $C(T)$ are temperature dependent functions. At 322K, $B(T) = 14.826 \text{ cc/mol}$ and $C(T) = 331.8 (\text{cc/mol})^2$.

For the designs considered, the re-entrant groove offers the best combination of heat transport capacity at adverse tilt and inherently lower internal pipe pressures due to its larger vapor/liquid volume ratio. The latter results in much smaller reservoir volume requirements for reducing internal pressures during storage. Assuming a design pressure of 100 atm and equal vapor volumes and tube dimensions, a re-entrant groove heat pipe would require an excess vapor reservoir volume about one-fifth of that needed for an artery or slab wick design, and less than half of that needed for a rectangular groove.

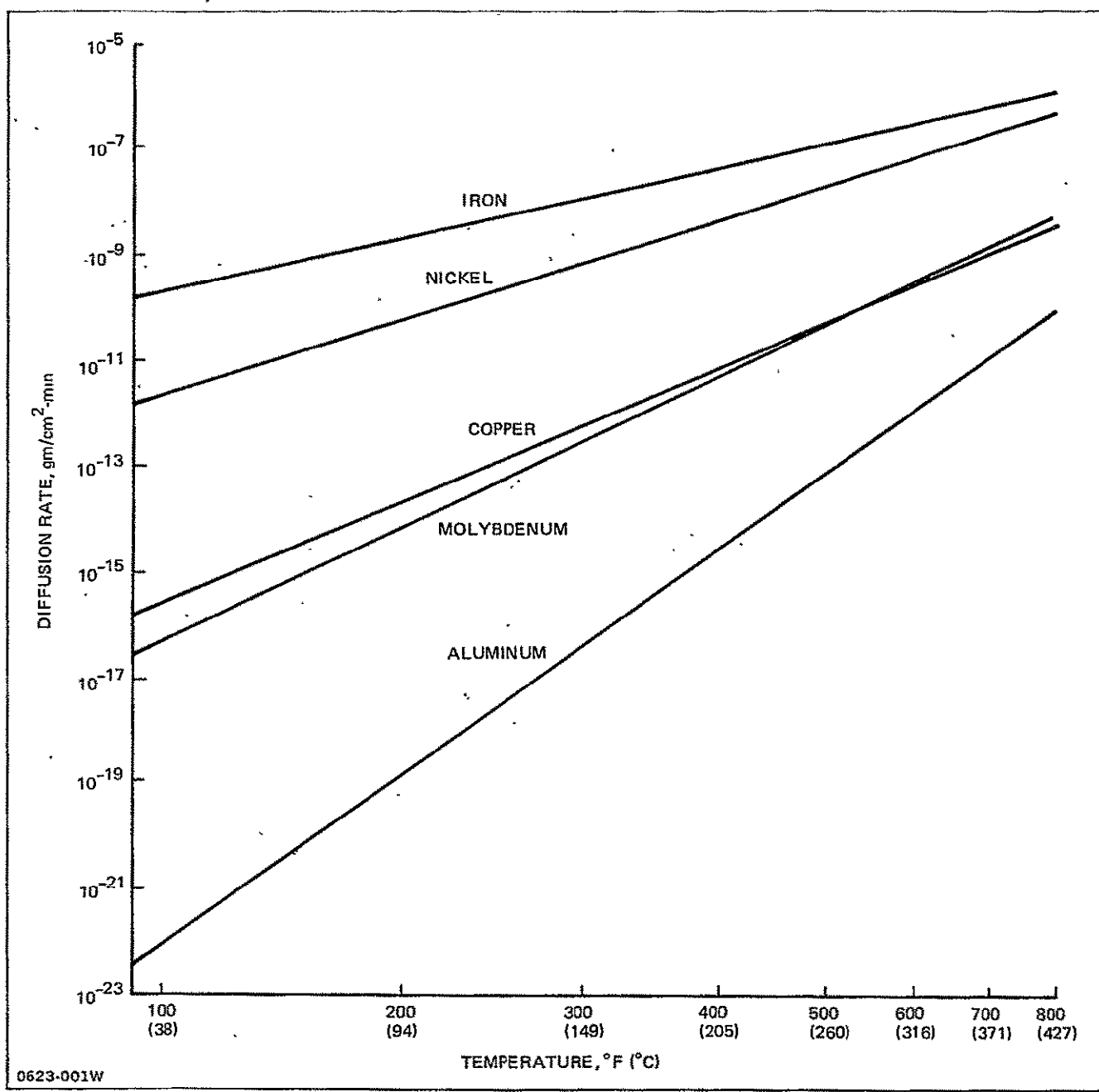


Fig. 1 Diffusion of Hydrogen Through Metals (Reference AEC Report AE61-1151)

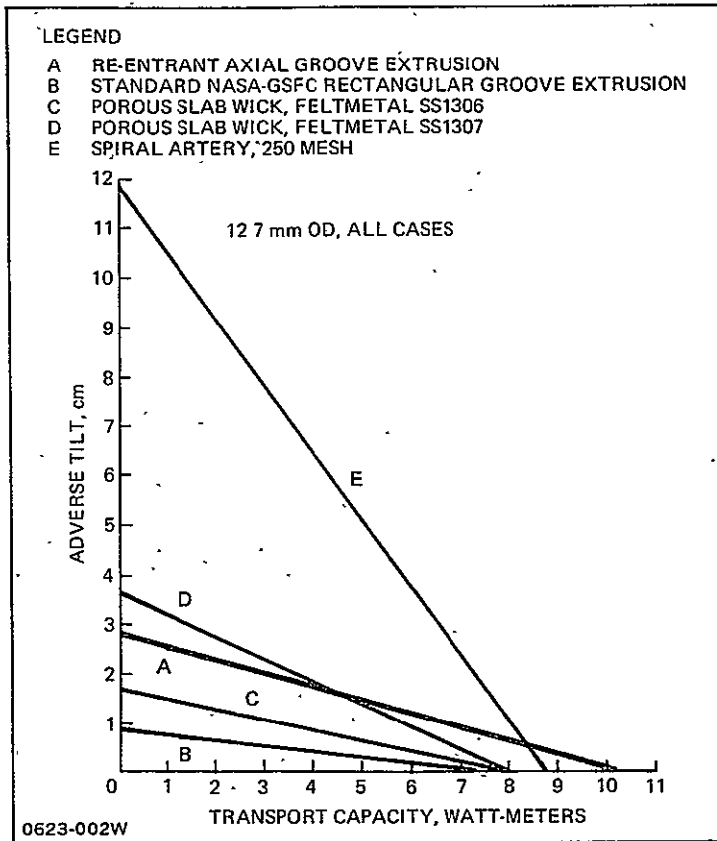


Fig. 2 Performance Comparison of Candidate Wicking Systems (Hydrogen @ 20 K)

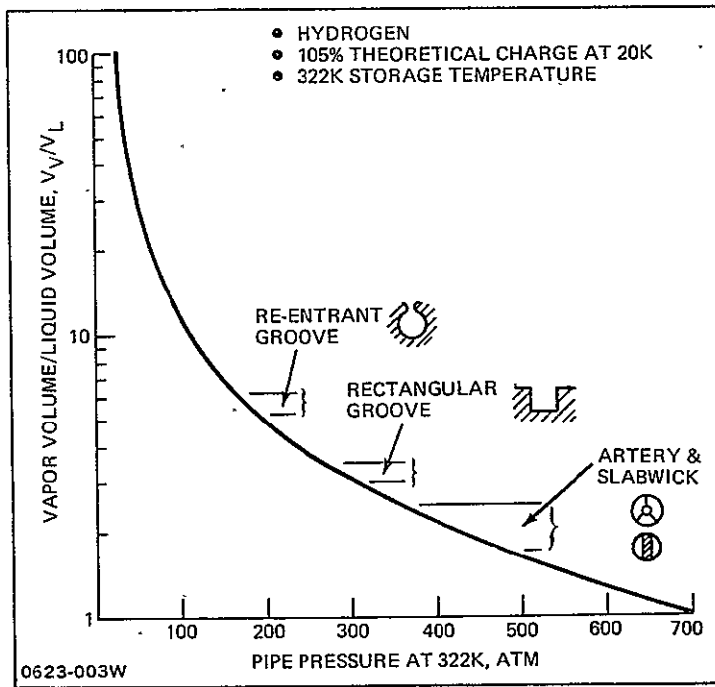


Fig. 3 Pressure Containment vs Volume Ratio

Since the re-entrant groove requires only 3/5 of the fluid charge of the standard rectangular groove it is more sensitive to an undercharged condition. But by the same token, its larger vapor/liquid volume ratio makes it less sensitive to an overcharge, i.e., burst pressure.

A secondary benefit of the re-entrant profile is the relatively narrow groove opening which exposes less liquid surface to the counterflowing vapor stream. This cuts down both liquid entrainment losses and vapor/liquid shear pressure losses, especially at the very low vapor pressures associated with operation near the triple point of hydrogen, where these phenomena become more pronounced.

A final consideration, and one which generally benefits axially grooved extrusions, is that the design fluid charge is more predictable and repeatable from pipe to pipe. This is because the other wick designs are more difficult to reproduce to close tolerances and are also more sensitive to liquid fillet contributions, which effectively increase the liquid volume.

PRECEDING PAGE BLANK NOT FILMED

Section 4

PARAMETRIC STUDY OF RE-ENTRANT GROOVE GEOMETRIES

The re-entrant groove geometry assumed for this study is shown schematically in Figure 4. The geometry can be defined by specifying the number of grooves (N), pipe outside radius (R_o), wall thickness (T), fin minimum thickness (S), fin edge radius (R_f), and minimum groove width (W). From these, the groove radius (R_g) and the pipe inside radius to the fin tip (R_i) can be determined. Alternatively, for some calculations, R_g can be specified and T determined.

The shape description is similar to that of the earlier NASA-Lewis extrusion⁴, differing only in having a constant fin edge radius, R_f , to form the neck of the groove. Discussions were held with the extruder, and it was felt that this change, plus limitations on minimum values of S , T , R_f , and W of 0.889, 0.610, 0.140 and 0.203 mm (0.035, 0.024, 0.0055 and 0.008 in.) respectively, would improve fabricability.

With these design constraints, a study was made of zero-g thermal transport capacity and pressure containment at 322 K (120°F) for variations in N , R_o , R_g , and for wall thickness values greater than the minimum. For the transport capacity calculations, the meniscus radius of curvature was assumed to equal R_i in the condenser, and $W/2$ in the evaporator.

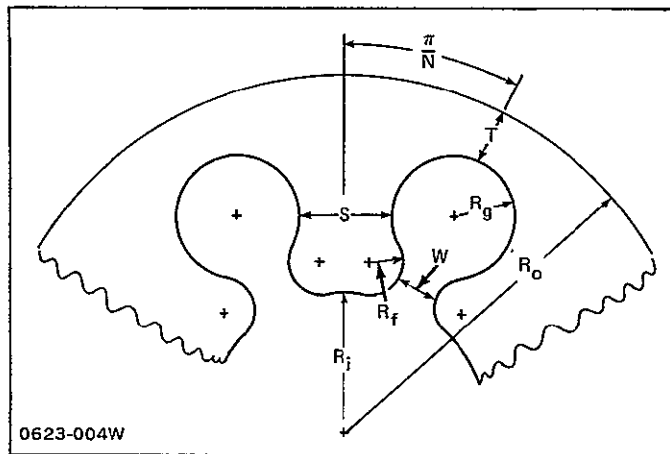


Fig. 4 Re-Entrant Groove Geometry Used for Parametrics

Transport capacity (Q_L) was computed from the relation

$$\overline{Q_L} = \frac{\left(\frac{2}{W} - \frac{1}{R_i} \right)}{\frac{32}{N_1 A_1 D_1^2} + \frac{32}{N_v A_v D_v^2}}$$

with liquid and vapor areas (A_1 and A_v) based on the arithmetic mean of the extreme condenser and evaporator groove fill conditions. The hydraulic diameters for the liquid and vapor flows were taken to be $2R_g$ and $2R_i$, respectively. N_1 and N_v are the zero-g figures of merit (surface tension, times latent heat divided by kinematic viscosity). The vapor shear term is neglected, but should be very small for most of the cases considered.

Pressure containment when the pipe is non-operational at relatively warm ambient conditions can be handled either by making the wall sufficiently thick or by providing a vapor expansion reservoir. The reservoir would have to be open to the pipe vapor space, not connected to any of the grooves, and located at or near the evaporator end of the pipe to assure that the reservoir only contains vapor when the pipe is operating. For a specified wall thickness, T , and allowable wall tensile stress, σ_a , the maximum pipe pressure is

$$P_{max} = \frac{T\sigma_a}{(R_o - T)}$$

The mean density of fluid within the pipe (with no fluid reservoir) is

$$\bar{\rho} = \frac{(\rho_1 A_1 + \rho_v A_v)C}{(A_1 + A_v)}$$

where C is the ratio of actual to theoretical charge (generally $C > 1$).

For the $\bar{\rho}$ value, the supercritical storage pressure P_{STOR} can be calculated for the maximum specified storage temperature and compared with P_{max} . In this study, the supercritical pressure calculations were made using an available computer subroutine based on the Benedict-Webb-Rubin equation⁶. For $P_{STOR} > P_{MAX}$, new values of $\bar{\rho}$ were determined by iteration to get $P_{STOR} = P_{MAX}$. The reservoir volume required per unit of pipe length was then calculated from

$$\frac{V_{RES}}{L} = \frac{C(\rho_1 - \bar{\rho})}{(\bar{\rho} - C\rho_v)} A_1 - A_v$$

Alternatively, if no reservoir is to be used, the wall thickness can be increased to make $P_{MAX} = P_{STOR}$.

The computer code which was written to permit the parametric solution of these equations is contained in Appendix A. Given predetermined constant values for the critical dimensions (S , T , R_f and W) the program evaluates both zero-g heat transport capacity and reservoir volume requirements for specified variations in N , R_o or R_g . The desired option is selected by the appropriate value of the input variable, Kt .

$Kt = 0$ vary pipe OD with all internal geometry constant

$Kt = 1$ vary number of grooves (and groove diameter) with pipe OD and wall thickness held constant

$Kt = 2$ vary number of grooves (and wall thickness) with pipe OD and groove diameter constant

$Kt = 3$ vary number of grooves (and fin thickness) with pipe OD, groove diameter and wall thickness held constant

$Kt = 4$ vary number of grooves, geometry is constant except groove diameter is chosen so that an excess vapor storage reservoir is not needed.

Some results obtained with this method of calculation are shown in Figures 5 through 8. All results shown are for pipes with hydrogen working fluid, a design operating temperature of 20 K, a design storage temperature of 322 K, and have minimum values of S , R_f , and W of 0.889, 0.140, and 0.203 mm, respectively. The pipes are assumed to have a maximum allowable yield stress of 8250 psi. For the minimum wall thickness of 0.610 mm and a pipe OD of 12.7 mm (0.50 in.), Figure 5 shows the effects on transport capacity and reservoir requirement of varying the number of grooves between 8 and 20. The 20 groove design is similar to the NASA Lewis extrusion, with a transport capacity of a little over $8W\text{-}m$, and a reservoir requirement of $155 \text{ cm}^3/\text{m}$. Reducing the number of grooves permits the groove diameter to be increased, raising transport capacity but also increasing the charge and associated reservoir requirement. Peak capacity occurs with 11 grooves. For less than 11 grooves, the vapor pressure drop becomes excessive, and transport capacity falls off. Because of the large reservoir requirement, these designs are not considered attractive.

Figure 6, which is also for a 12.7 mm OD pipe, shows the effects of varying wall thickness while keeping groove diameter constant at 0.785 mm. The 20 groove case is identical with that of Figure 5. Reducing the number of grooves below 20 results in a near linear fall off in transport capacity. Reservoir volume requirements drop very rapidly as the number of grooves is reduced, since charge is decreasing as wall thickness is increasing. For 16 or fewer grooves, no reservoir is needed.

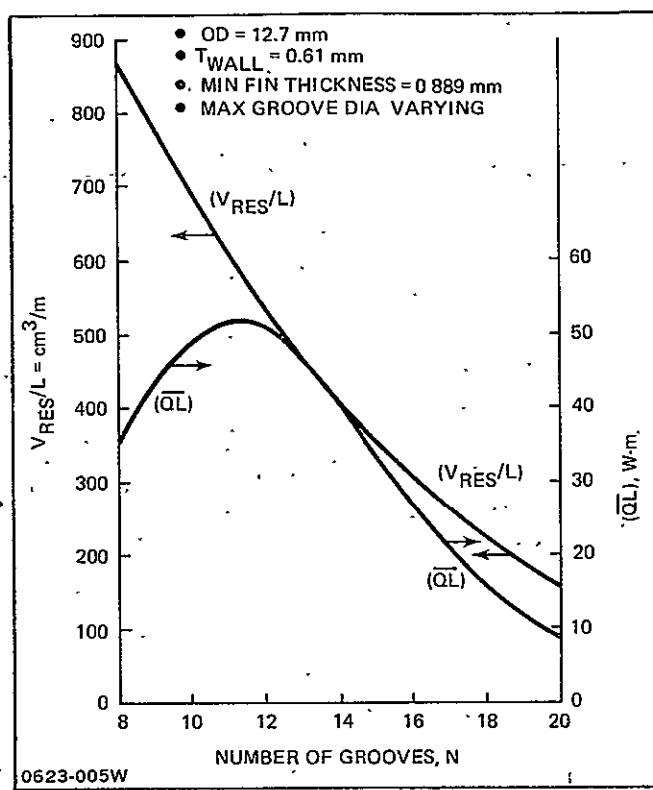


Fig. 5 Transport Capacity and Reservoir Volume vs Number of Grooves for Constant Wall Thickness

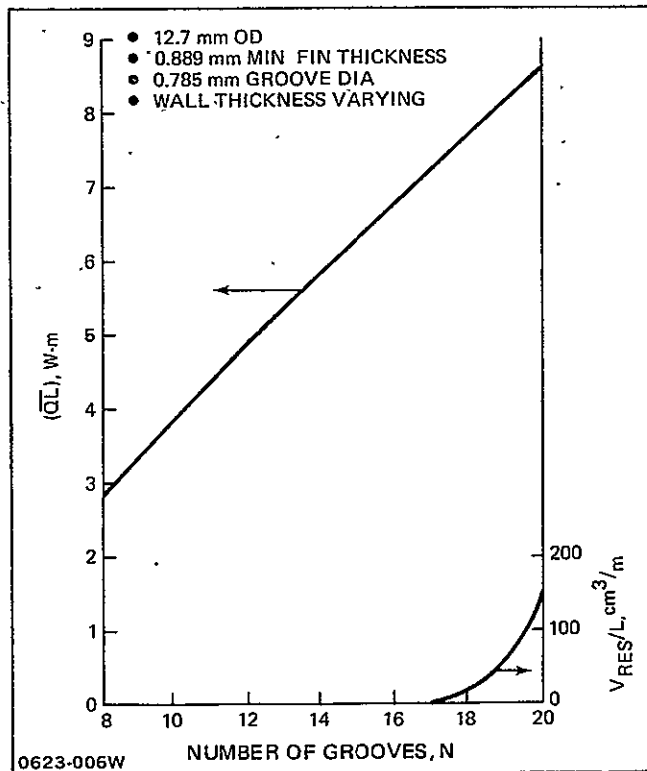


Fig. 6 Transport Capacity and Reservoir Volume vs Number of Grooves for Constant Groove Diameter

Figure 7 shows the effect of varying outside diameter on the reservoir requirement and the wall thickness, keeping a constant number of grooves (20) and a constant groove diameter (0.785 mm). In effect, this keeps the pipe ID and internal geometry constant, so that all these cases have a transport capacity of about 8 W-m. As shown, the reservoir requirement reduces to zero for a pipe outside diameter of 14.6 mm (0.575 in.).

Figure 8 shows transport capacity for a number of designs all with thick enough walls to contain storage pressure without a reservoir. Transport capacities as high as 11, 18, and 25 W-m are predicted for pipe outside diameters of 12.7, 14.6, and 15.9 mm, respectively. These results should be treated with some caution, however, since the high transport capacities are associated with relatively large diameter grooves, and may have relatively low evaporator heat flux limitations.

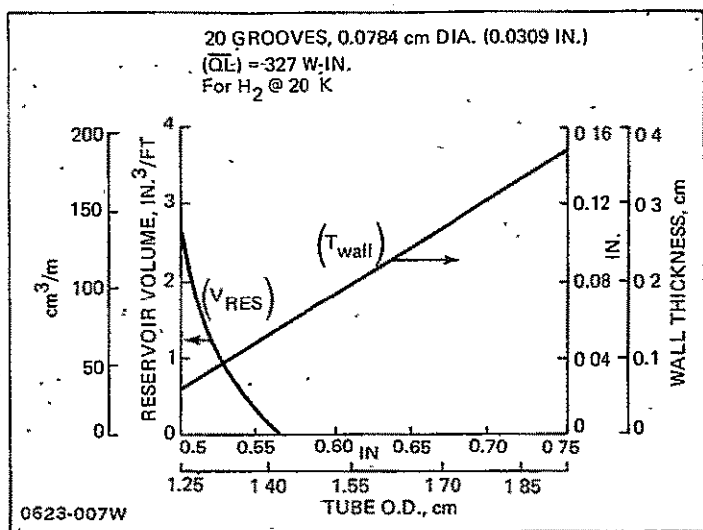


Fig. 7 Effect of Increasing Outside Diameter, Keeping Inside Geometry Constant

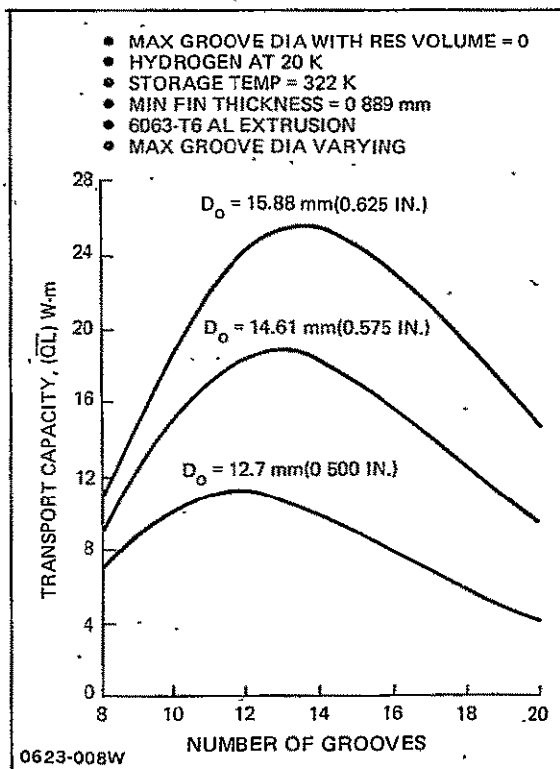


Fig. 8 Transport Capacity vs Number of Grooves with Wall-Thickness Adequate to Eliminate Reservoir

PRECEDING PAGE BLANK NOT FILMED

Section 5

DESCRIPTION OF THE RE-ENTRANT GROOVE EXTRUSION

5.1 THE EXTRUSION

The design which was specified to the extrusion vendor, Micro Extrusions, attempted to keep the basic groove characteristics of the original NASA-LeRC re-entrant profile with minor changes meant to improve fabricability. Primarily, the keyhole passageway was replaced with smoothly rounded fin tips at the groove opening. The outside diameter was also increased to minimize reservoir volume requirements, while still keeping a manageable size and a reasonable chance of obtaining a successful extrusion. The specified design geometry to be produced from 6063 Aluminum is shown in Figure 9. These nominal dimensions were used for the performance predictions previously given in Figure 2. It may be noted from Figure 7 that these nominal dimensions, if achieved, would eliminate the need for a vapor reservoir.

Initial production efforts proved very difficult and resulted in broken dies and limited lengths of extrusion having a 14.4 mm OD and a 1.37 mm wall thickness. All groove channels were elliptical (eccentricity ≈ 0.55), smaller than specified, and three of the twenty grooves had wider, malformed groove openings due to three die teeth which had broken immediately. Most important, the passageways of the intact grooves were keyhole shaped, similar to the NASA-LeRC extrusion, with a nominal groove opening of 0.25 mm at the tip. New, slightly modified dies were prepared for a second attempt, which proved successful in all but one respect. While the groove neck region now had the desired rounded shape, the openings were about 50% larger than specified. But this adjustment permitted extruding over 100 meters of tubing without a die failure.

The characteristic dimensions of the second re-entrant groove extrusion were determined by following the methods of Harwell⁴.

- Random micrometer measurements of the outside tube diameter along its length and around its circumference
- Internal volume measurements by carefully weighing sample lengths of tubing first empty and then filled with water
- Photomicrograph enlargements of 2 cm long samples which were cut from the heat pipe extrusion, mounted in epoxy, and polished to expose the sharp groove profile.

Figure 10 shows enlarged photographs of one of the samples. The characteristic dimensions of the tube and grooves as measured from this 20X enlargement are reported in Table 1, along with a pictorial explanation.

The internal cross sectional areas of the actual heat pipe tube were computed from measured data taken from samples of the same extruded length.

Method	Computed Area (mm ²)		
	Total Void	Vapor Core	Grooves (20)
Dry Weight Measurement	83.33	69.7	13.63
Vol of Water to Fill Tube	83.25	69.7	13.55

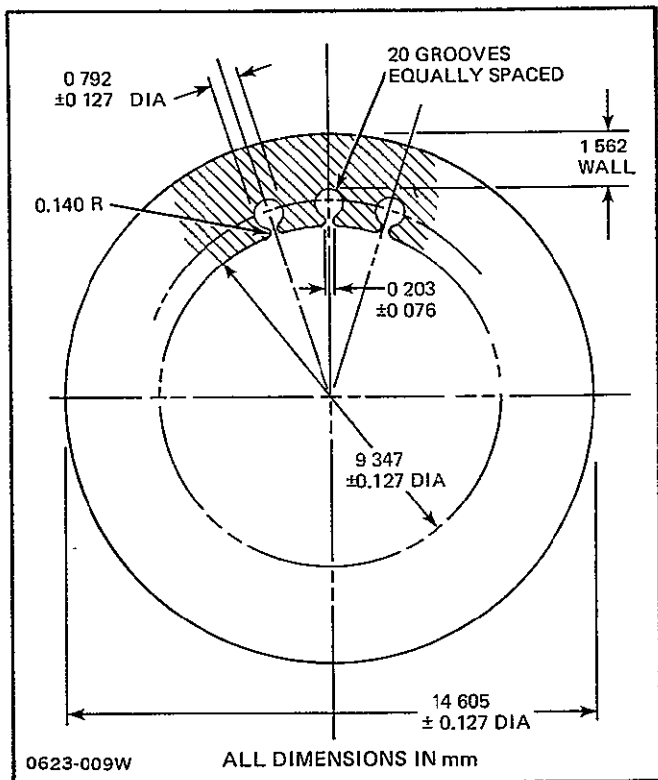
These data, which are more conservative than the measured dimensions, were used to calculate the 105% theoretical fluid charge and the resulting excess vapor reservoir requirement for storage pressure containment.

5.2 THEORETICAL PERFORMANCE

Two different computer codes were used to predict the theoretical heat pipe performance; AXIAL - a code developed in Reference 4, and GAP - a code developed in Reference 7. Both programs account for the vapor/liquid shear loss in addition to the normal viscous pressure drops in the liquid and vapor channels. Input data for both was based on the nominal dimensions, as measured from the photomicrograph enlargement. Results for both ammonia at 20°C and hydrogen at 20 K are given below.

	Hydrogen (20 K)		Ammonia (20°C)	
	Axial	Gap	Axial	Gap
Zero-g Transport Capacity (W-m)	5.3	6.8	136.2	155.3
Static Wicking Height (cm)	1.7	1.65	2.13	1.93
Theoretical Fluid Charge (g)	0.872	0.955	7.19	7.88

The primary difference between these predictions for the "as-extruded" heat pipe and the earlier one for the "as-specified" geometry can be explained by the slightly narrower groove channel diameter (0.77 mm vs 0.79 mm) and the wider groove opening (0.33 mm vs 0.20 mm). The former accounts for about 15 percent of the difference and the latter, about 85 percent.



ORIGINAL PAGE IS
OF POOR QUALITY

ORIGINAL PAGE IS
OF POOR QUALITY

Fig. 9 Specified Design Geometry

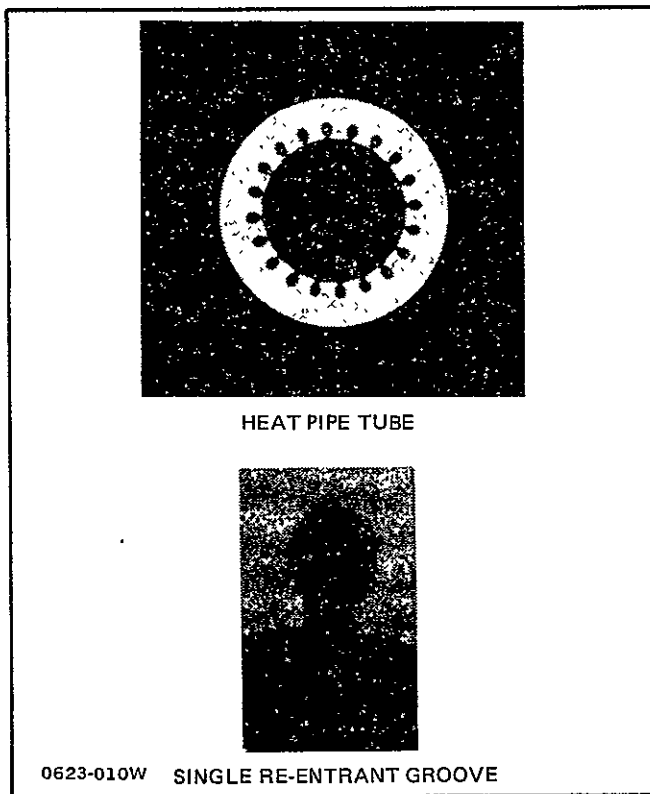
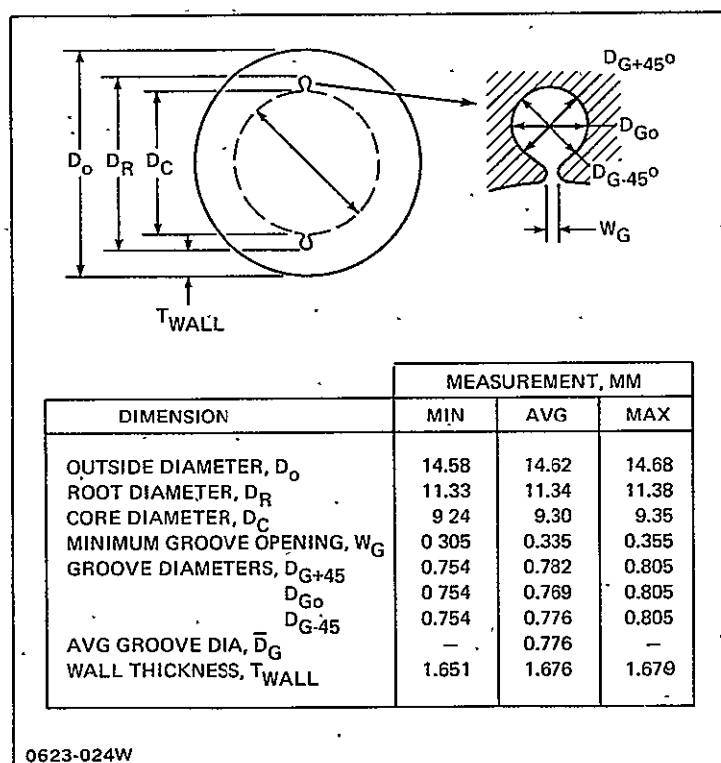


Fig. 10 Photomicrograph of Re-Entrant Groove Extrusion

Table 1 Characteristic Dimensions of the Hydrogen Heat Pipe Extrusion



5.3 STORAGE PRESSURE CONTAINMENT

A review of the burst test data for other heat pipe extrusions made from 6063 Aluminum and fabricated in a similar manner indicates that failure usually occurs near the endcap weldment, even after heat treatment to a T-6 condition. Table 2, which summarizes this data, also shows the calculated values for the ultimate tensile strength, as determined by test data. They are about 5000 psi less than the published value of 30,000 psi for 6063-T6 extruded tubing. Based on this pressure test data, an allowable design stress of 6250 psi (25 percent of the ultimate stress) was used to determine a maximum allowable storage pressure of 109 atm (1600 psi). Note that this is lower than the 8250 psi used in the earlier parametric studies. Burst test samples of the actual re-entrant groove tubing, but without representative end weldments, failed at 6450 psi, giving an ultimate strength of 24900 psi ($17.2 \times 10^7 \text{ N/m}^2$).

Since a vapor/fluid volume ratio of 10.5 is needed to decrease the internal pipe pressure to 109 atm (refer to Fig. 3), an excess vapor reservoir of 117 cc was required. The reservoir is made from thick walled 6061-T6 aluminum tubing and contains no internal wicking system. It is located at the evaporator end of the 100 cm long heat pipe and is attached to it by swageloc fittings. This permits the reservoir to be removed when testing other cryogenic fluids that do not require extra vapor volume.

Table 2 Burst Pressure Test Results for 6063 Aluminum Axially Grooved Extrusions

EXTRUSION	OD (mm)	ID (mm)	$T_{WALL/R}$	BURST PRESSURE		BURST LOCATION	$\bar{\sigma}_{ULT} = \frac{P_{BURST}}{(t/R)}$		
				atm	PSI		$N/m^2 \times 10^{-7}$	PSI	
1. NASA-GSFC T-6 AS WELDED	a)	12.01	10.72	0.116	241	3550	PIPE	20.9	30 279
	b)	12.7	10.72	0.169	395	5800	PIPE	23.6	34 279
	c)	13.41	10.72	0.223	391	5750	WELD	17.8	25 762
	d)	14.22	10.72	0.281	510/ 626	7500/ 9200	WELD	18.4/ 22.6	26 684/ 32 740
2. GRUMMAN FLANGED AXIAL GROOVE T-6 AS WELDED	e)	14.12	10.67	0.278	401/ 462	5900/ 6800	WELD	14.6/ 16.9	21 223/ 24 460
3. NASA - LeRC T-6 TUBE, NO END WELD 0623-025W	f)	12.6	11.33	0.106	190	2800	—	18.2	26 376

PRECEDING PAGE BLANK NOT FILMED

Section 6

HEAT PIPE DESIGN AND FABRICATION

The design of the basic heat pipe is similar to that detailed in Reference 4, except for dimensional changes needed to accommodate the thicker wall, larger OD tubing. In addition to the extruded tube, the primary heat pipe components are the seal rings, which prevent end wall drainage during ground test, and two end caps (one configured with an integral charge tube) which are welded to the tube ends. The charge tube is positioned at the evaporator end of the pipe to preclude any inadvertent accumulation of fluid which would starve the heat pipe and cause premature dryout.

Attached to the heat pipe charge tube is the excess vapor reservoir, which itself has a charge tube. A secondary charge tube is also attached to the reservoir. After filling the pipe, the secondary charge tube is pinched-off and welded closed. The heat pipe can then be tested in a sealed condition without the charge valve. This eliminates a potential source of fluid leakage during the low temperature tests and eliminates the need for an excessive amount of trace heat which might be required to keep the valve at a high enough leak tight temperature.

The manufacturing sequence which was followed is summarized in Figure 11. The final heat pipe assembly (after charging and pinch off) is shown in Figure 12.

6.1 CHARGE REQUIREMENT

Test results for the hydrogen heat pipe with ammonia (see Par. 7.2) indicate that 8 grams is the 100 percent ammonia fluid charge at 20°C. The measured vapor core area is 0.697 cm² and the corresponding liquid area, based on the 8 gram ammonia charge, is found to be 0.1302 cm² for the 100 cm long heat pipe section. These measurements were taken without the excess vapor volume attached to the evaporator end of the heat pipe. When used with hydrogen, an excess vapor volume of 117.46 cc is needed to reduce storage pressures below the allowable limits. Thus, the total void volume of the hydrogen heat pipe is 200.19 cc, comprised of the following:

$$\begin{aligned} V_{\text{void}} &= V_{\substack{\text{vapor} \\ \text{core}}} + V_{\text{liquid}} + V_{\text{reservoir}} \\ &= (A_V + A_L) L + V_{\text{res}} \\ &= (0.697 + 0.1302) (100) + 117.46 \end{aligned}$$

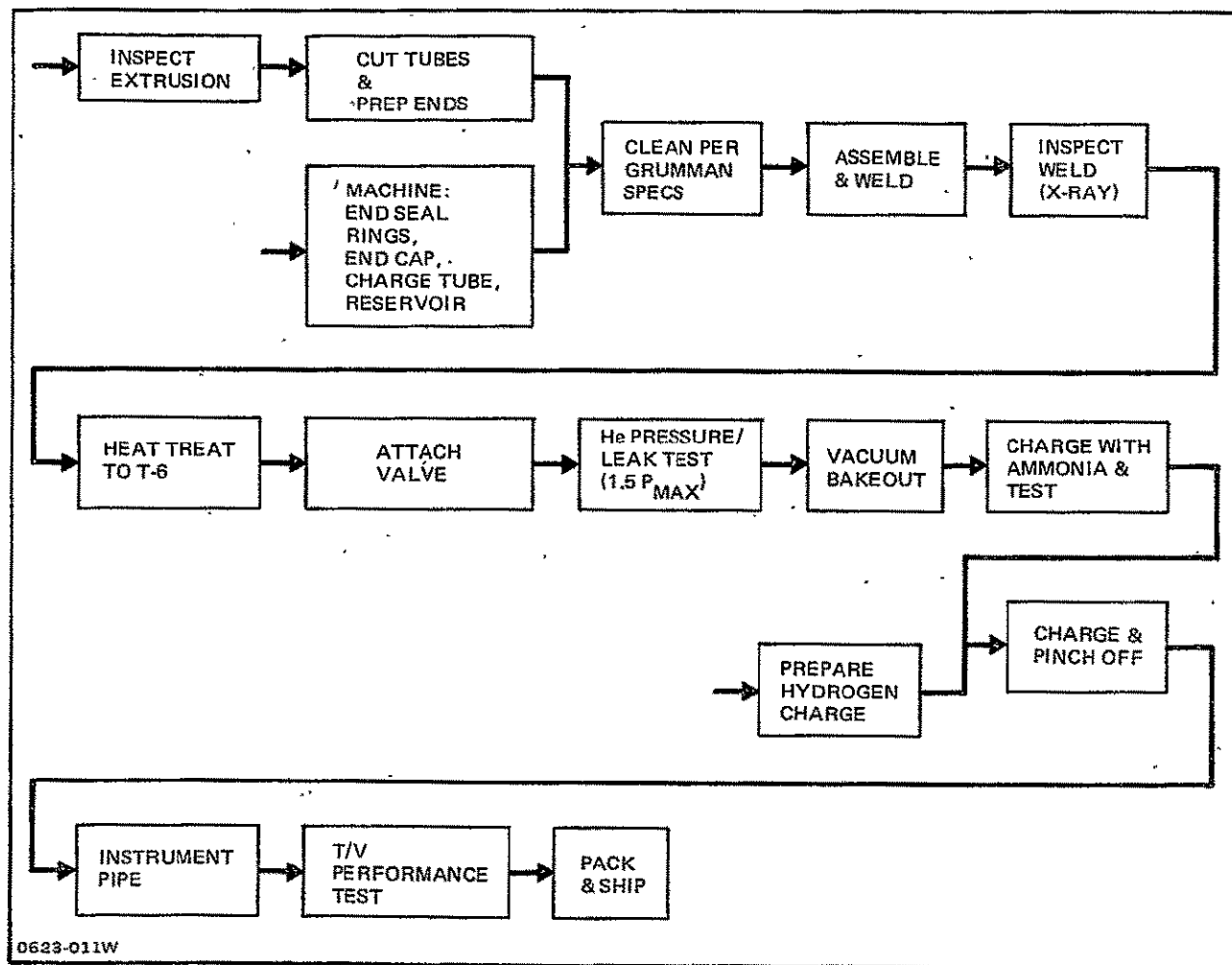


Fig. 11 Manufacturing Plan for Hydrogen Heat Pipe

ORIGINAL PAGE IS
OF POOR QUALITY

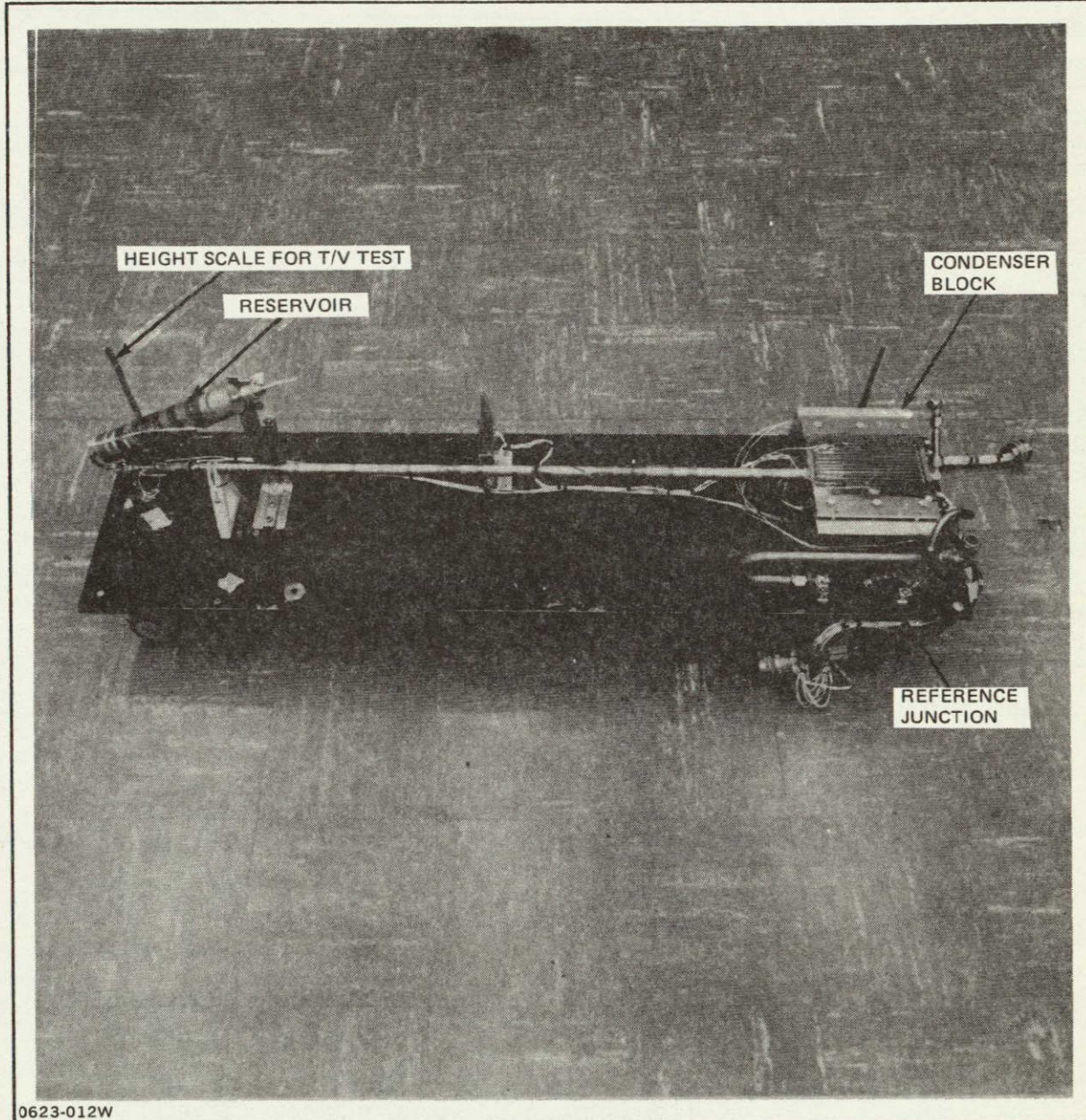


Fig. 12 Hydrogen Heat Pipe Final Assembly, on Test Stand

$$V_{\text{void}} = 200.19 \text{ cc}$$

The required hydrogen charge at the 20 K design point is based on the aforementioned volumes and a 5 percent overcharge of the heat pipe.

Thus,

$$M = (\rho_L A_L L + \rho_V A_V L) (1.05) + \rho_V V_{\text{res}}$$

where $A_L = 0.1302 \text{ cm}^2$, $A_V = 0.697 \text{ cm}^2$, $L = 100 \text{ cm}$, $V_{\text{res}} = 117.46 \text{ cm}^3$ and for hydrogen at 20 K, $\rho_L = 0.07156 \text{ g/cc}$ and $\rho_V = 0.001187 \text{ g/cc}$. Upon substitution, $M = 1.2 \text{ grams}$ of hydrogen.

6.2 CHARGE PROCEDURE

The charging procedure is based on a superheated vapor technique where the charge in the pipe is determined by measuring the pressure of the known heat pipe void volume (200.19cc).

Using the virial equation of state:

$$P = RT \bar{\rho}(\varphi)$$

where $\varphi = (1 + B(T) \bar{\rho} + C(T) \bar{\rho}^2)$ and $R = 0.08206 \text{ atm-l/g-mol K}$, $T = \text{temperature}$

(K), $\bar{\rho} = \text{density (mol/cc)}$ and $B(T)$ and $C(T)$ are temperature dependent functions.

At 322 K, $B(T) = 14.826 \text{ cc/mol}$ and $C(T) = 331.8 (\text{cc/mol})^2$.

For $M = 1.2 \text{ g}$, $V_{\text{void}} = 200.19 \text{ cc} \rightarrow \rho = 0.005994 \text{ g/cc}$

$$\text{and } \bar{\rho} = \rho / M_w = \rho / 2.016 = 0.002973 \text{ mol/cc.}$$

Therefore, $\varphi = 1 + 14.826 (0.002973) + 331.8 (0.002973)^2$

$$\varphi = 1.047$$

$$P = 82.06 (322) (0.002973) (1.047)$$

$P = 82.24 \text{ atm} = 1209 \text{ psia}$, maximum internal storage pressure.

Values at room temperature (297 K) are:

$$P = 1114 \text{ psia for } m = 1.2 \text{ g}$$

and

$$P = 921 \text{ psia for } m = 1.0 \text{ g}$$

thus the sensitivity = 96.5 psi for every 0.1 grams in this range.

The setup and procedure used for charging the heat pipe with hydrogen are shown in Figure 13. The steps are as follows:

1. Install hydrogen supply bottle, hydrogen pressure regulator and the heat pipe to the vacuum chamber as shown in Figure 13. The supply bottle pressure is 1585 psig. (1.09 E07 Pa).
2. Go to high vacuum. Keep valve A closed. Open valves B, C and D and evacuate system.
3. Close valves B and C and open supply bottle valve A.
4. Open primary side of valve B, then secondary side, as necessary, to get 1100 psig (7.58 E06 Pa) pressure in system (Note: 1100 psig corresponds to required 1.2 g charge).
5. Close heat pipe valve D and valve A.
6. Crack fitting at secondary side of valve B while purging with nitrogen gas. Remove fitting and purge all lines with nitrogen. Cap fitting closed, open valve C to vent system.
7. Remove heat pipe; pinch off and weld.

Note: Due to a total system volume that was slightly larger than anticipated, the heat pipe was charged to 1075 psig (7.41 E06 Pa), which was the maximum attainable system pressure with the 1585 psig (1.09 E07 Pa) supply bottle.

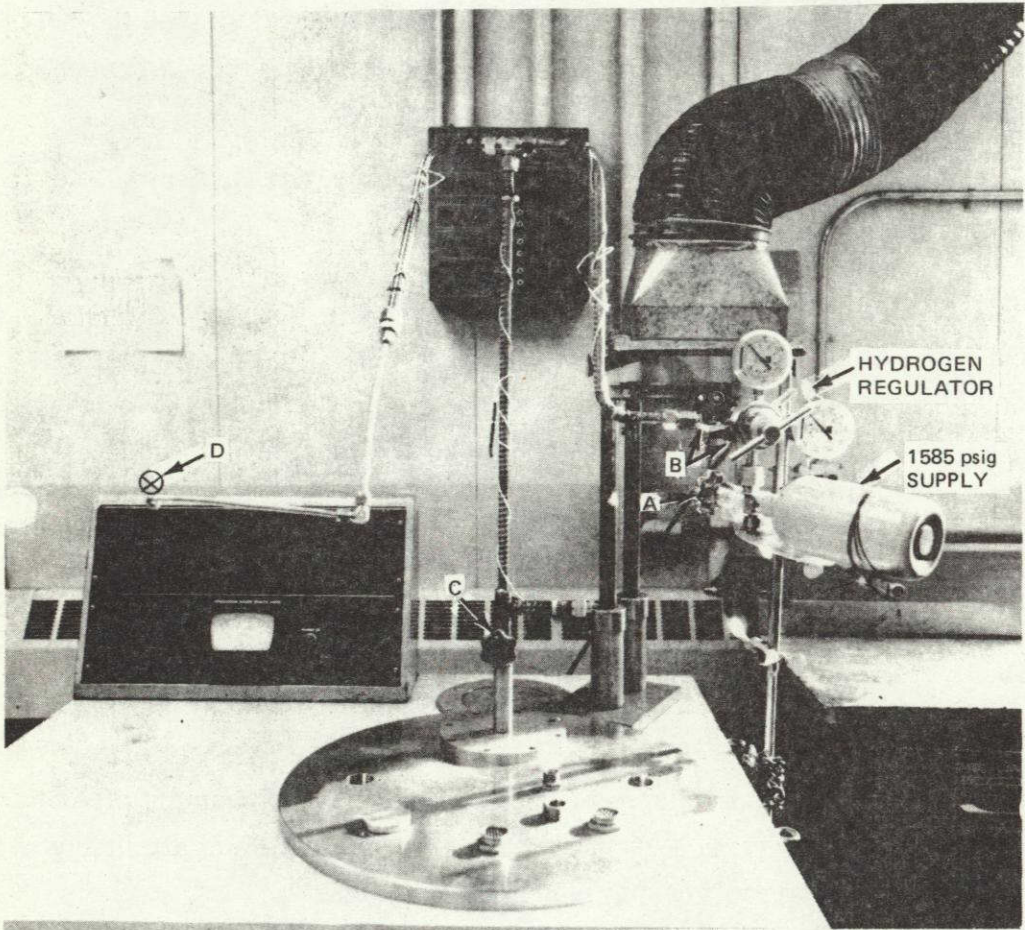
6.3 STRENGTH CHECK

6.3.1 Heat Pipe

The allowable stress for the heat pipe extrusion is 5000 psi (3.45 E07 Pa). Using the hoop stress formula with a wall thickness of 1.676 mm and radius of 6.49 mm, the allowable internal storage pressure is 1291 psi (8.9 E06 Pa). This exceeds the 1100 psi (7.58 E06 Pa) charging pressure and is therefore acceptable.

6.3.2 Reservoir

For the reservoir (6061-T6) the allowable stress is 6000 psi (4.1 E07 Pa). The wall thickness and radius are 3.96 mm and 17.07 mm, respectively. The resulting allowable pressure is 1392 psi (9.6 E06 Pa) which also exceeds the requirement. Note: The reservoir and walls are 1.27 cm thick to prevent endwall failure (See Reference 8).



NOTES:

1. ALL TUBING 1/2 IN. OD (3/8 IN. ID)
2. SYSTEM AT ROOM TEMP (75° F)

PROCEDURE

1. EVACUATE LINES AND HP
2. ADD CHARGE TO HP
3. VENT SYSTEM AND REMOVE HEAT PIPE

0623-013W

Valves			
A SUPPLY	B REGULATOR	C VACUUM STA	D HEAT PIPE
C	O	O	O
O	O	C	O
C	O	O	C

LEGEND:
O = OPEN
C = CLOSED

Fig. 13 Charging Set-Up/Procedure for Hydrogen HP

Section 7

TEST EVALUATION

The heat pipe was first tested in a room temperature environment with varying charges of ammonia working fluid. In addition to obtaining ammonia test data, these tests were used to accurately determine the optimum fluid charge so that the heat pipe could be properly filled with hydrogen. For each measured ammonia charge, the maximum heat transport capacity was determined as a function of adverse tilt.

Once the proper charge had been determined, the heat pipe was filled with research purity hydrogen and tested in a thermal vacuum chamber using a liquid helium cooling system. The hydrogen test program was designed mainly to develop a performance map for the heat pipe, which consisted of tilt/dryout data at nominal operating temperatures.

7.1 INSTRUMENTATION

The location of all instrumentation was the same for both the ammonia and hydrogen test programs, although by necessity the composition of the thermocouple wire was changed. Copper/constantan wire was used for the room temperature tests, and Chromel vs Gold -0.07 at. %Fe was used for the hydrogen tests because of its superior sensitivity. A comparison with other possible thermocouple materials over the temperature range 10 to 25 K is given below.

Thermocouple Wire	Sensitivity ($\mu\text{V/K}$)
Chromel-Alumel	3.0
Copper-Constantan	4.0
Chromel-Constantan	6.5
Chromel-Gold-Iron	16.8

The instrumentation layout for the heat pipe is shown in Figure 14. A total of 10 thermocouples, each positioned at the 3 o'clock orientation, were used on the heat pipe proper: four each on the evaporator and condenser sections and two on the transport section. Two thermocouples were located on the heat pipe charge tube so that the heat transfer from the reservoir could be measured. Two more thermocouples monitored the reservoir temperature to insure that it was always slightly warmer than the evaporator. A trace heater was attached to the reservoir so that any liquid trapped in it could be vaporized and returned to

the heat pipe. However, since reservoir temperature was never a problem, it was never used during the tests.

In addition to these primary temperature measurements, a limited number of copper-constantan thermocouples were used for backup, although they were never actually needed. One was located on the evaporator (7.5 cm from the end), one on the transport section, and two on the condenser block.

Electrical heat input was supplied to the evaporator by Nichrome ribbon, which was helically wrapped and attached to the pipe by a 1/2-mil layer of double-backed Kapton tape. A second layer of single-backed Kapton tape insulated the heater from the surroundings. The thermocouples at the evaporator were attached directly to the pipe wall with the bead located between consecutive turns of the heater. All thermocouples were bonded in place with EA 934 adhesive. To minimize stray emf due to thermal gradients, several turns of thermocouple wire were taken before the wire was routed to the ambient.

The accuracy of the low temperature measurements was enhanced by avoiding large temperature gradients between the ends of the thermocouple junctions. Therefore, each leg of the Chromel-Gold wire was referenced to an LN₂ cooled cold junction, as indicated in the thermocouple schematic of Figure 15. In this case, the reference junction was a copper tube through which LN₂ was routed after it left the primary cold wall of the thermal vacuum chamber. The thermocouple junctions were electrically insulated by a layer of Kapton.

A temperature resolution of better than 0.1 K was obtained using a direct-reading, high resolution, precision potentiometer (Leeds and Northrup Type K-3 Universal Guarded Potentiometer, which had a resolution of 0.5 μ V per division). This was used to measure the thermocouple emf. Since the Chromel vs Au - 0.07 at. %Fe has a test range sensitivity of 16 μ V/K, the 1.6 μ V emf output for each 0.1 K was well within the required measuring capability.

7.2 TESTS WITH AMMONIA

The primary purpose of this test was to confirm the theoretical (100 percent-fill) charge for the re-entrant groove heat pipe so that the optimum hydrogen charge could be accurately determined. In addition, complete performance maps (Q vs tilt) were generated, and repriming behavior from both mechanical and mechanical/thermal dryout was observed.

7.2.1 Test Setup

For the ammonia tests the heat pipe was configured without the reservoir, and the charge valve remained attached to the heat pipe assembly since the fluid charge was suffi-

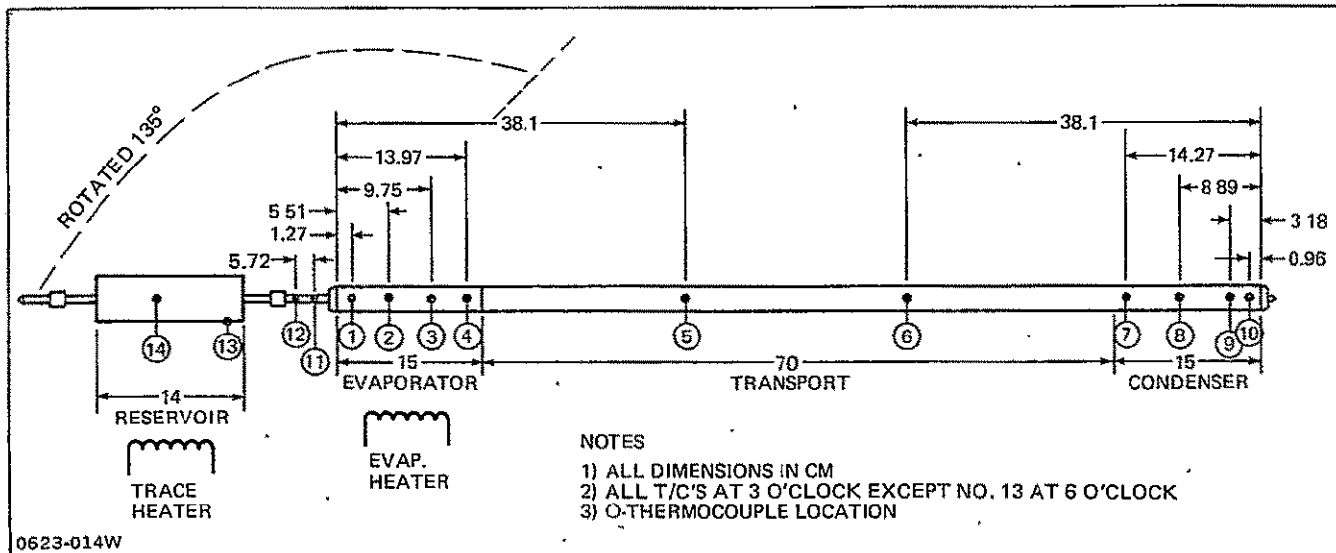


Fig. 14 Heat Pipe Test Instrumentation

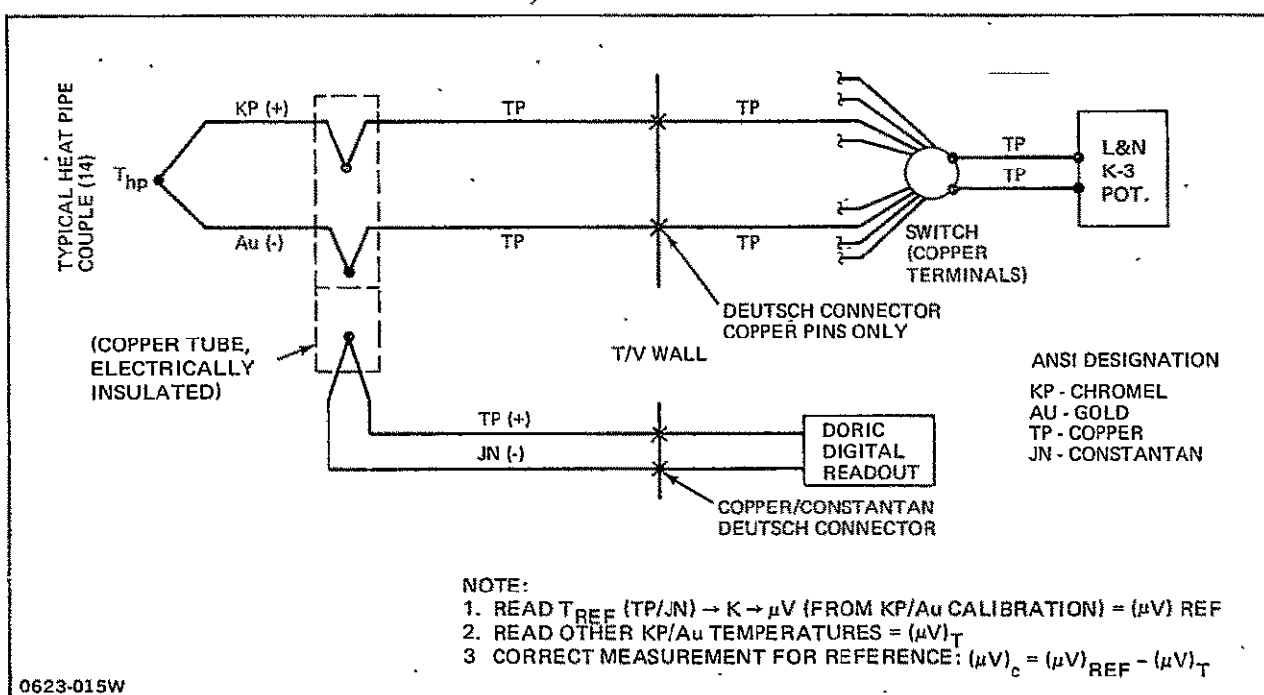


Fig. 15 Low Temperature Thermocouple Schematic

ciently large (≈ 9 g) that it had little effect on heat pipe performance. The pipe was mounted on a standard laboratory test stand that had the capability of accurate adverse tilt adjustments from level to 7.6 cm (3.0 in.), and up to at least 15 cm (6 in.) when the heat pipe had to be disabled. Testing was done in a room temperature environment with a cold water spray bath used as the condenser heat sink. The remainder of the heat pipe, including valve, was completely surrounded with Armaflex insulation. The Cu/Con thermocouples were continuously monitored with a multipoint Bristol chart recorder, while the steady-state temperature distributions were recorded using a Doric digital voltmeter. Evaporator heat input was regulated by a Variac, and the power was measured using an ammeter and voltmeter.

7.2.2 Results

The maximum heat transport vs adverse tilt performance maps for selected ammonia charges are summarized in Figure 16. The change of slope near zero tilt values signals a liquid puddle contribution, and is indicative of an excess fluid charge. As seen, the 8 gram charge resulted in the highest heat transport (130 watts) without evidence of a puddle. The lower 7.5 gram charge had a concave shape and lower heat transport, which indicates an undercharged condition. Corresponding film heat transfer coefficient data are given in Figure 17. They indicate unexpectedly low values of 2014 and $5362 \text{ W/m}^{20^\circ\text{C}}$ for the evaporator and condenser, for an equivalent overall heat pipe conductance of $5.85 \text{ W/}^\circ\text{C}$. Performance comparisons with the standard rectangular groove and the original keyhole re-entrant groove data are given below.

Groove Configuration	Heat Transport Capacity (W-m)	Static Wicking Height (cm)	Film Heat Transfer Coefficients ($\text{W/m}^{20^\circ\text{C}}$)	
			Evaporator	Condenser
Rounded Tip Re-entrant	110	1.65	2014	5362
Rectangular	127	1.20	8681	9504
"Keyhole" Re-entrant (Ref. 4)	143	2.51	7300	20,500

Tests to monitor recovery from a mechanical/thermal dryout were also run with an 8.5 gram ammonia charge. The adverse tilt was first raised to 17 cm. Then, 7 watts of power were applied for several minutes so that the evaporator temperature exceeded the condenser temperature by 25°C . The heat pipe tilt was then decreased to 1.27 cm (1/2 inch), and the evaporator power was set at a lower value than that previously determined for Q_{\max} . Results indicated that the heat pipe recovered heat pipe operation at heat loads up to 60 per-

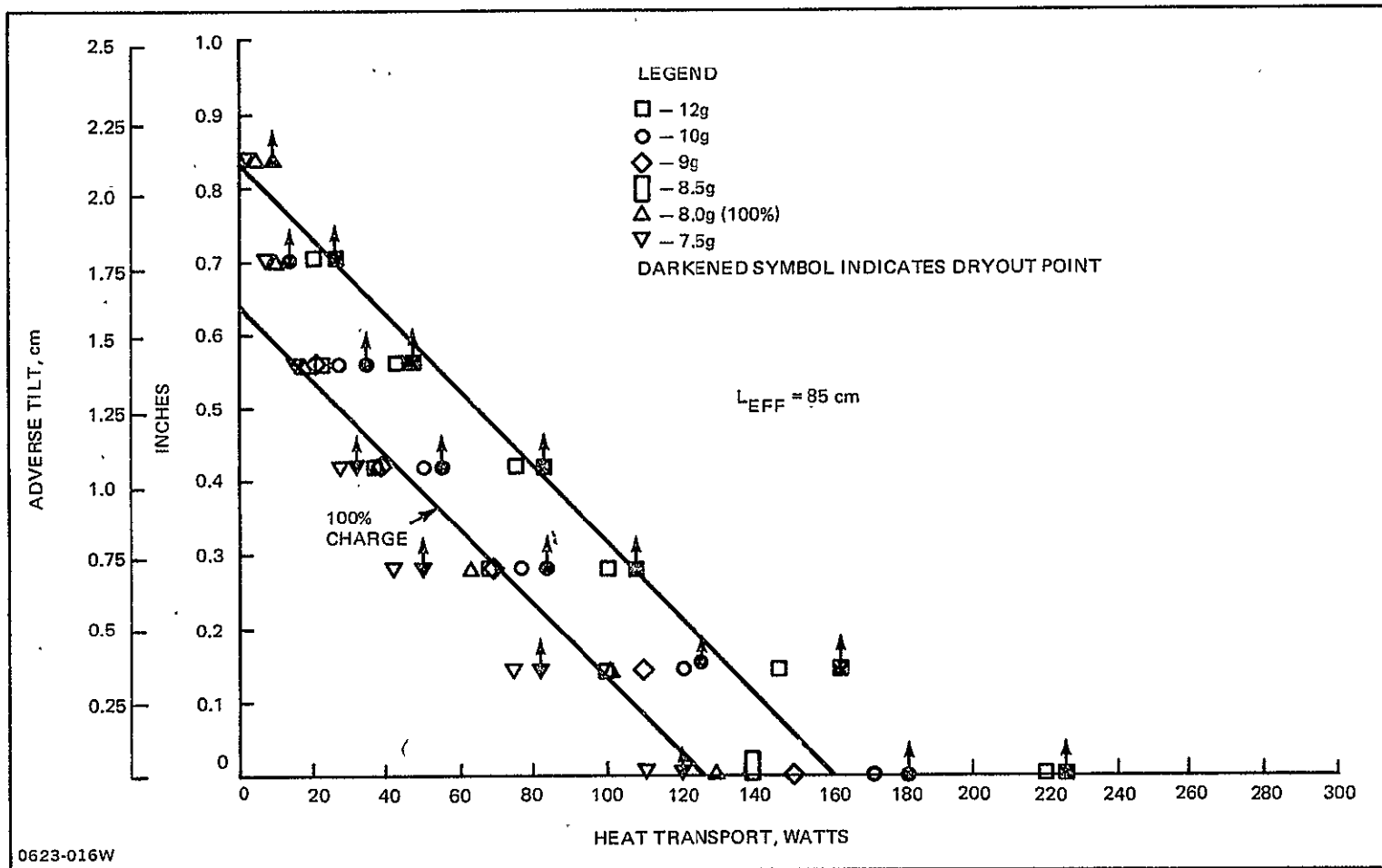


Fig. 16 Performance of NASA-AMES Re-Entrant Groove Heat Pipe with Ammonia @ 20°C

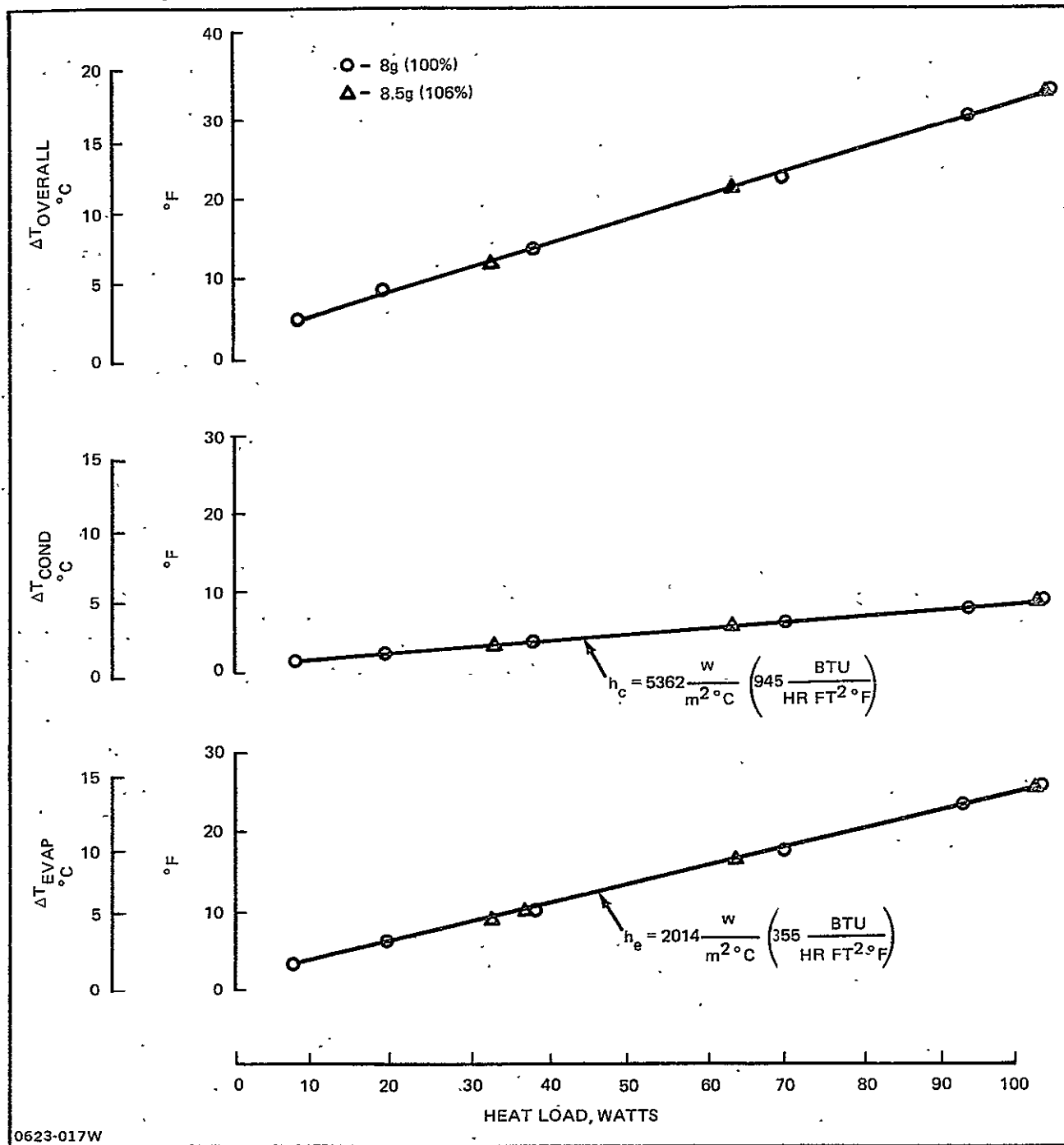


Fig. 17 Re-Entrant Groove Extrusion with Ammonia, Temperature Gradients

cent of the Q_{max} value, as evidenced by the convergence of the evaporator temperature towards the condenser temperature.

7.3 TESTS WITH HYDROGEN

The hydrogen test program was designed mainly to develop a performance map for the heat pipe at the nominal 20 K operating temperature. This consisted of first setting an adverse tilt, then incrementing the evaporator heat input until dryout occurred. Performance at selective off-design temperatures was also measured. The associated temperature profiles were used to determine the overall heat pipe conductance. Recovery of heat pipe operation after a thermal dryout was also monitored. A test point, with the evaporator severely raised to prevent heat pipe operation, was included to determine the effect of heat conduction through the aluminum tube at cryogenic temperatures. A secondary test objective was to examine the transient response of the pipe during cooldown from room temperature, during freeze-out and during thaw.

7.3.1 Test Setup

All tests with hydrogen fluid were run in a specially modified end-loaded thermal vacuum chamber (60 cm in diameter by 122 cm long) located in the plant 14 Thermal Lab. Condenser cooling was provided by a liquid helium cooling system. As shown in Figure 18, the chamber contained an MLI-backed LN_2 cold wall as the primary means of thermal isolation from the room environment. A regenerative copper cold wall, which was cooled by escaping helium boiloff from the condenser block, served as a secondary thermal barrier. All chamber feedthroughs, except the LN_2 cold wall, are through the removable end wall, which also contains a 7.6 cm diameter viewing port. The heat pipe test assembly, including the condenser cooling block, was mounted on a 1.27 cm thick aluminum plate and isolated from it by low thermal conductance Teflon standoffs. The entire test assembly was encased in 30 layers of aluminized mylar multilayer insulation: the condenser block had a double blanket, or 60 layers.

The chamber was balanced on a knife edge and supported by precision jack stands, so that tilt adjustments of up to 7.6 cm could be made by tilting the entire chamber. A surveyor's transit and metering scales, attached to opposite ends of the pipe assembly and viewed through the window, were used to accurately measure differences in elevation. Although never used, external metering scales were also mounted to the ends of the chamber as a backup, in case the internal view was obscured. A comparison and correlation between the two readings was made, using LN_2 coolant in the cold walls and cooling block, and indicated a stable platform.

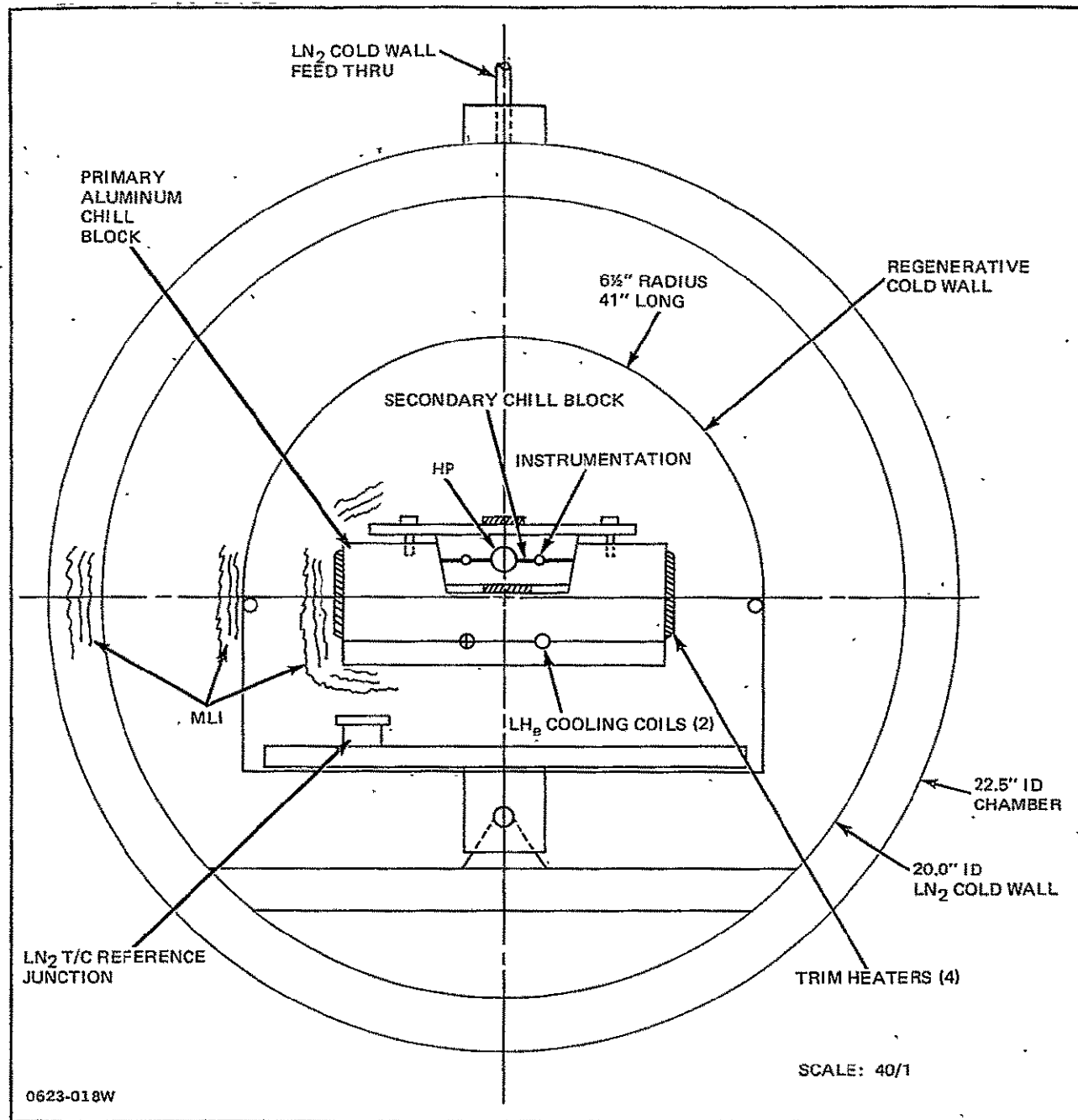


Fig. 18 Low Temperature T/V Chamber Test Set-Up – End View

The condenser section of the heat pipe was firmly squeezed between the two parts of a split dove-tailed aluminum chill block, which were bolted together. Shallow channels, which were machined into the mating faces of the block in both axial and transverse directions, served as conduits for the thermocouple wires. The temperature of the chill block (and the heat pipe) was controlled by an aluminum cooling block to which it was conductively coupled. This primary cooling block contained both liquid helium flow channels and electrical trim heaters. The latter were never needed. Additional trim heaters were attached directly to the smaller chill block. These were the only ones actually used to stabilize heat pipe test temperatures.

The desired nominal operating temperature for the heat pipe was established by adjusting the trim heaters on the chill block after a stable helium flow rate had been established. A near-constant heat pipe operating temperature was maintained by decreasing the trim heater input in accordance with the incremental increases in evaporator heat load. All electrical heat inputs were determined by measuring the actual voltage and amperage, which accounted for any variations in electrical resistance.

The helium cooling system (see Figure 19) was supplied by an expendable 500 ℓ liquid helium dewar, which was connected to the chamber feedthroughs by vacuum jacketed transfer lines. A stable helium flow rate as high as 12 liters/hour was maintained by pressurizing the dewar to 2.5 psig with gaseous helium, and then adjusting the flow control valve on the dewar. To permit accurate flow measurements, and as a safety precaution to prevent the formation of liquefied air, an inline heater was used to pre-heat the helium vapor to about 300 K before venting to the atmosphere. The vent line was also fitted with a thermocouple and a calibrated flow meter, so that the boiloff rate could be measured and flow adjustments made to compensate for excessive liquid helium blow-through. During most test points, the actual helium usage nearly matched the theoretical rate required by the electrical power dissipations. This indicates a very efficient cooling system, with minimum losses due to either blow-through or extraneous heat leaks.

For instance, the following values were recorded for a typical test point (Day 3-7-79, time 0637 hrs):

Evaporator Heater = 3.5 watts (8.3V, 0.422a)
Trim Heater = 4.3 watts (7.05V, 0.61a)
Helium Gas Flow Rate = 50 percent at 50[°]F (283K)

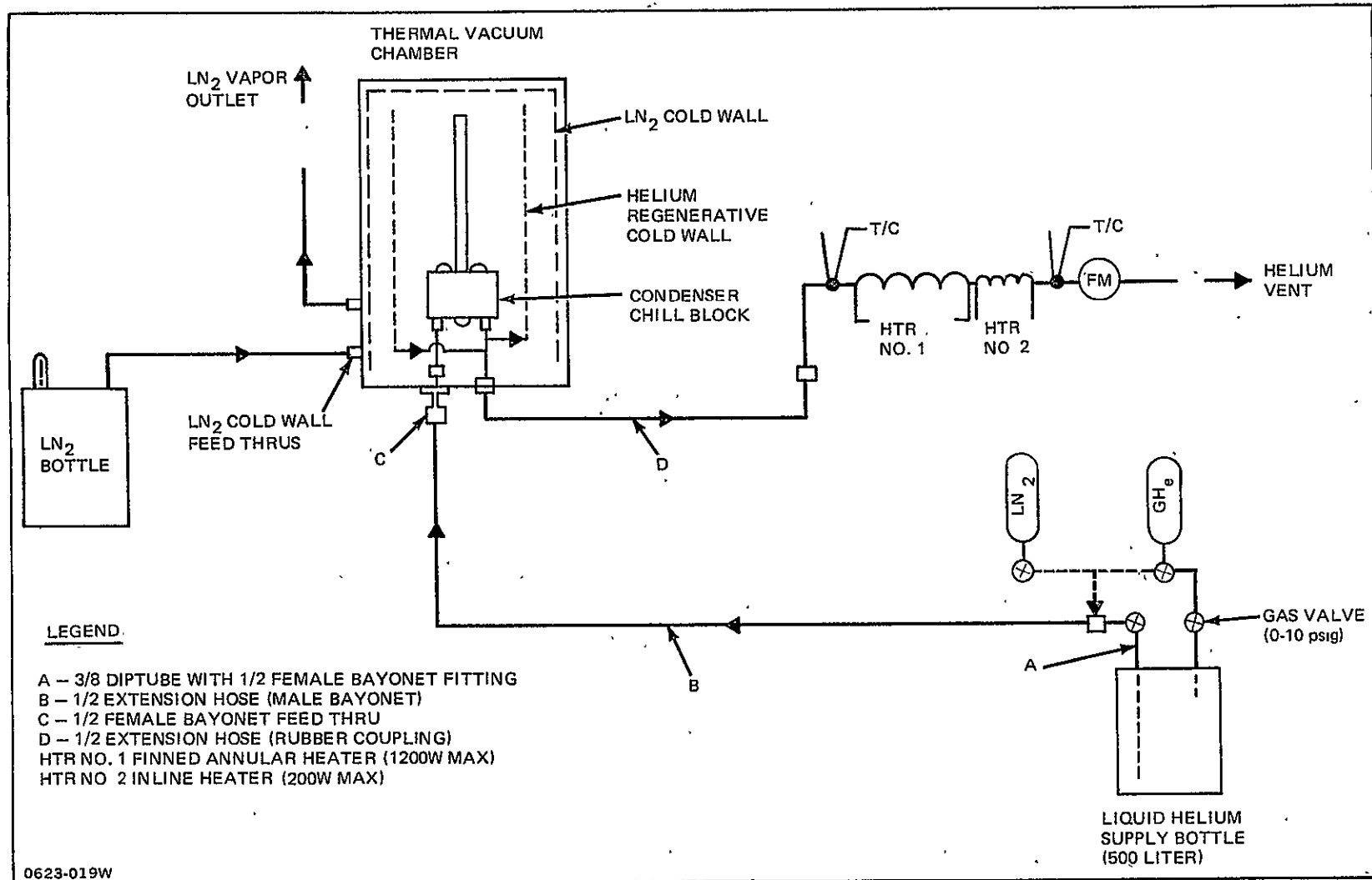


Fig. 19 Flow Schematic — Low Temperature Facility

- Actual Helium Flow Rate (Typical)

At a 50 percent scale reading the calibration curve for the flow meter indicates 1.6913 scfm of air. This is corrected for helium gas by the following relationship:

$$(\bar{A}\bar{V})_{He} = \left(\frac{\rho_{air}}{\rho_{He}} \right)^{\frac{1}{2}} (\bar{A}\bar{V})_{air}$$

where $(\bar{A}\bar{V})$ indicates the volumetric flow rate and ρ is the corresponding density.

Thus the corresponding helium gas flow rate is (using engineering units):

$$\begin{aligned} (\bar{A}\bar{V})_{He} &= \left(\frac{0.07493}{0.01074} \right)^{\frac{1}{2}} (1.6913) \\ &= 4.467 \text{ cfm} \end{aligned}$$

The liquid helium flow rate is then given by:

$$\begin{aligned} (\bar{A}\bar{V})_L &= \left(\frac{\rho_V}{\rho_L} \right) (\bar{A}\bar{V})_V \\ &= \left(\frac{0.01074}{7.84} \right) \frac{4.467}{(0.035)} (60) \\ (\bar{A}\bar{V})_L &= 10.49 \text{ liters/hour} \end{aligned}$$

- Ideal Flow Rate

The ideal flow rate is the boil off rate that exactly equals the electrical power requirements. For a total dissipation of 7.8 watts, the ideal flow rate is calculated as follows:

$$\begin{aligned} (\bar{A}\bar{V})_L &= \frac{Q}{\rho_L \lambda} \\ &= \frac{(7.8) (3.413)}{(7.84) (8.9) (.035)} \\ (\bar{A}\bar{V})_L &= 10.9 \text{ liters/hour} \end{aligned}$$

To minimize helium waste, the condenser cooling block was initially cooled from room temperature using liquid nitrogen. Gaseous helium was then used to vent any nitrogen from the lines before the liquid helium was introduced. The startup cooling procedure used is contained in Appendix C.

- Tare Heat Leaks

Before liquid helium cooling was actually used, an experimental heat leak tare test was run with liquid nitrogen as the coolant. The block was first cooled to 77 K, then the liquid nitrogen flow was stopped, and the remaining LN_2 residue was purged with nitrogen gas until the block reached 88 K. At that point a known amount of electrical heat (10.6 watts)

was input to the primary heaters and the temperature rise of the block was measured with time. Over a period of 25 minutes, the block temperature increased from 83.0 K to 90.8 K, an average rate of 18.7 K per hour. The tare leak can then be estimated by solving the following heat balance:

$$Q_e + Q_L = (MC_p) \frac{dT}{d\tau}$$

where Q_e = electrical heat input = 10.6 watts

Q_L = tare heat leak

(MC_p) = thermal capacitance of the condenser block

($dT/d\tau$) = average temperature rise rate

The condenser block assembly weighs 5.45 Kg (12.0 lbs) and the average value of heat capacity for aluminum over this temperature range is 0.093 cal/gm^oC. Thus, the capacitance of the block is 506.9 Cal/^oC (1.116 Btu/^oF). Solving for the unknown heat leak yields:

$$Q_L = (MC_p) \frac{dT}{d\tau} - Q_e$$

$$Q_L = 0.41 \text{ watts}$$

The corresponding average temperature difference measured between the condenser block and the mounting plate during the tare test was 50.5 K (90.8^oF). Thus, an equivalent heat leak conductance for these temperature levels can be estimated as $0.41/50.5 = 0.0081$ watts/^oC (0.0045 watts/^oF). The important assumption implicit in this value is that conduction heat leaks predominate over radiation.

Other factors to be considered are changes in thermal conductivity that occur between the liquid nitrogen tare test and the actual liquid helium test temperatures. For instance, between 90 K and 20 K the conductivity of Teflon (the standoff material) decreases from 0.233 to 0.147 watts/m^oC (0.135 to 0.085 Btu/hr ft^oF), while that of copper (instrumentation) increases from 493 to 1210 watts/m^oC (285 to 700 Btu/hr ft^oF). On the other hand, aluminum decreases from 221 to 182 watts/m^oC (128 to 105 BTU/hr ft^oF).

The theoretical heat leaks are comprised of the following:

- conduction through the Teflon standoffs (6 at the condenser block, one at the evaporator)
- radiation through the MLI (60 layers around the condenser block, 30 layers around the rest of the heat pipe assembly)
- conduction through the instrumentation (thermocouples and heaters)

- conduction from the reservoir through the charge tube and into the end of the evaporator. This leak is greatest at the start of testing when the reservoir is warm and decreases to a negligible amount with time.

The Teflon standoffs are described in Figure 20. At the condenser block, the average cross sectional area for a standoff is 1.15 cm^2 (0.179 in.^2) with an effective length of 3.81 cm (1.5 in.). The conductance of each teflon standoff at 90 K is then:

$$K \frac{A}{L} = 0.00070 \text{ W/}^\circ\text{C} (0.00039 \text{ W/}^\circ\text{F})$$

For the six standoffs, the total conductance is $0.0042 \text{ W/}^\circ\text{C}$ ($0.0023 \text{ W/}^\circ\text{F}$) where the temperature difference is measured between the condenser block and the mounting plate. Based on a cross sectional area of 2.016 cm^2 (0.3125 in.^2) and an effective length of 10.16 cm (4 in.) for each leg, the conductance through the evaporator support is calculated to be $0.0032 \text{ watts/}^\circ\text{C}$ ($0.0017 \text{ watts/}^\circ\text{F}$).

The total surface area of the condenser block is 1161 cm^2 (180 in.^2); the remainder of the heat pipe (evaporator and transport sections) has a surface area of 389.8 cm^2 (60.4 in.^2). During the tare tests, the average temperature of the regenerative cold wall was 116 K (-250°F), while the heat pipe assembly averaged 87 K (-303°F). Using an effective emittance of 0.01 for the MLI blanket, the overall radiation leak can be estimated as:

$$Q_{L,R} = \sigma A \epsilon_{\text{eff}} (\bar{T}_{HP}^4 - \bar{T}_S^4)$$

$$Q_{L,R} = 0.011 \text{ watts}$$

This value is much less than the measured heat leak of 0.41 watts , which validates the approach of neglecting radiation and treating the tare leak as a linearized conductance between the heat pipe assembly and mounting plate.

The instrumentation which is not attached directly to the heat pipe condenser or cooling block is routed along the heat pipe beneath the MLI. Since the overall length ranges from 122 to 152 cm , the associated heat leaks are negligible. However, the instrumentation attached to the cooling block assembly has much shorter transfer lengths. It consists of 8 thermocouple wires ($0.559 \text{ mm diameter each}$), 18 thermocouple wires (0.127 mm dia.), and 8 heater wires ($2.54 \text{ mm diameter each}$). To avoid excessive conduction leaks from the thermal vacuum chamber feedthroughs, both the heater wire and thermocouple harnesses are cold sunk (i.e., strapped) to the helium exit line coming from the regenerative cold wall. The 0.127 mm dia. thermocouple wires run between the cooling block and the LN_2 reference junction. In addition, all of the instrumentation harnesses and coolant lines were wrapped with 30 layers of MLI.

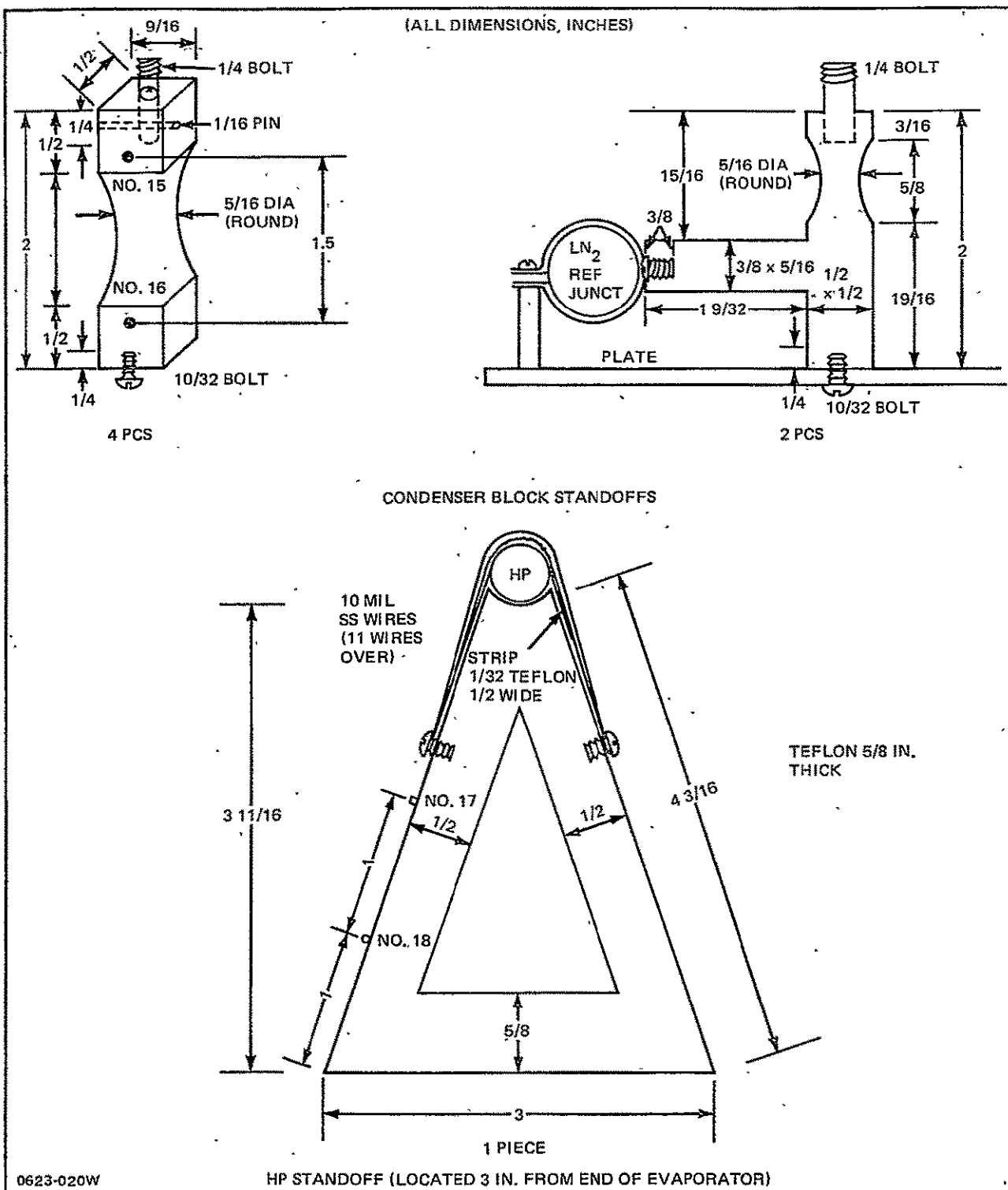


Fig. 20 Heat Pipe Assembly Standoff Supports (Mat'l Teflon)

Heat leak through the charge tube (Q_{ct}) was calculated from the known geometry. By measuring the temperature gradient along the tube, we find that:

$$Q_{ct} = K \frac{A}{L} (T_{12} - T_{11})$$

$$Q_{ct} = 0.019 (T_{12} - T_{11}), \text{ watts}$$

where the thermal conductivity is based on the value at 90 K and the temperature difference is in degrees centigrade. The charge tube heat leak was greatest at the start of testing, when the reservoir was relatively warm, but became negligible as the reservoir lost its stored thermal energy, which took about 3 hours.

The estimated heat leaks for both LN₂ cooling and LHe cooling are presented below. Tare test measurements were about 30 percent below theoretical which is reasonable considering the small magnitudes involved (<1W).

Summary of Heat Leak Estimates

	<u>LN₂ Cooling</u>	<u>LHe Cooling</u>
Measured at Condenser Block During Tare Test:	0.41w	--
<u>Theoretical Calculations</u>		
Mounting Plate to HP (Conduction):	0.36w	0.23w
Instrumentation: (Conduction)	0.21w	0.32w
MLI (Radiation):	0.01w	<0.01w
Charge Tube (Conduction):	--	0.60w → 0.0w
Total Theoretical:	0.58w	0.55w plus charge tube

7.3.2 Hydrogen Test Results

The cooldown transient for the hydrogen heat pipe (without an evaporator heat load) is presented in Figure 21, and shows the spread between selected evaporator, transport, and condenser temperatures at given times. The helium cooling rate averaged about 5 liters per hour, with various chillblock trim heater inputs used to stabilize the condenser temperature. Heat pipe action started about 2½ hours into the cooldown, as evidenced by the convergence of all three temperatures within the expected 15 to 33 K operating range.

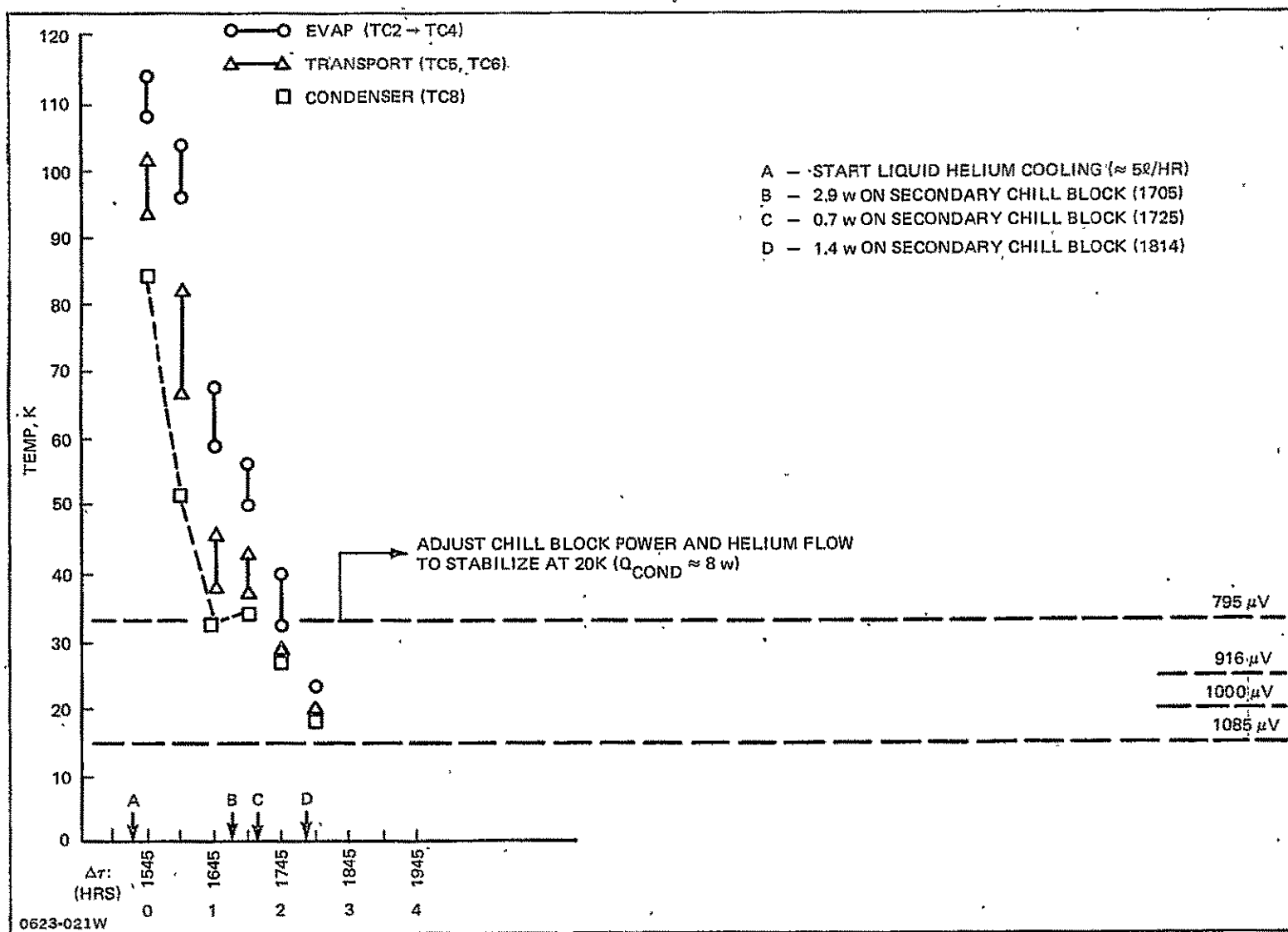


Fig. 21 Cool Down Transient

The steady state performance data were taken over a temperature range of 19 to 23 K. They are summarized in Figure 22 in a plot of net evaporator heat load versus heat pipe tilt. The data (solid line) indicate a static wicking height of 1.42 cm and a maximum transport capacity of 5.4 w-m. Predicted performance extrapolated from the ammonia test data is indicated by the dashed line. The static wicking height agrees with predictions, while the heat transport capacity is only 9.5 percent larger than anticipated. The errors associated with the measured data are <0.2 percent for the heat input and ± 0.063 cm (± 0.025 in.) for the tilt measurement.

The corresponding values for the overall average temperature gradient between the evaporator and condenser sections at each heat load are plotted in Figure 23. The variation is linear and indicates an overall heat pipe conductance of 1.7 W/ $^{\circ}$ C, which is 29 percent of the ammonia value. It is of interest to note that this is close to the variation in thermal conductivities between the two liquids, which is about 24 percent.

Detailed temperature profiles at the various tilt positions are presented in Figure 24. The measurements at the far ends of the heat pipe (1.27 cm at the evaporator and 0.96 cm at the condenser) have been omitted since they were suspect. Post-test examination showed that the evaporator thermocouple had lifted from the heat pipe wall, which would cause it to read higher than the rest of the evaporator. The thermocouple at the end of the condenser may be influenced by variations in clamping pressure, since it typically registered 1 to 2 $^{\circ}$ C warmer than the other condenser measurements.

Recovery of heat pipe operation after a dryout was no problem. Whenever a dryout was witnessed during a steady state test point, the evaporator heat load was reset to the previous value. The heat pipe always recovered operation within a few minutes.

As a final test, start up of heat pipe operation from a completely frozen condition was also successfully demonstrated. The heat pipe was kept frozen for three hours by holding the condenser at approximately 12 K. A 1.8 watt evaporator heat load was then applied, and within five minutes the heat pipe was operational at 15 K. The corresponding temperature profiles for the startup sequence are shown in Figure 25.

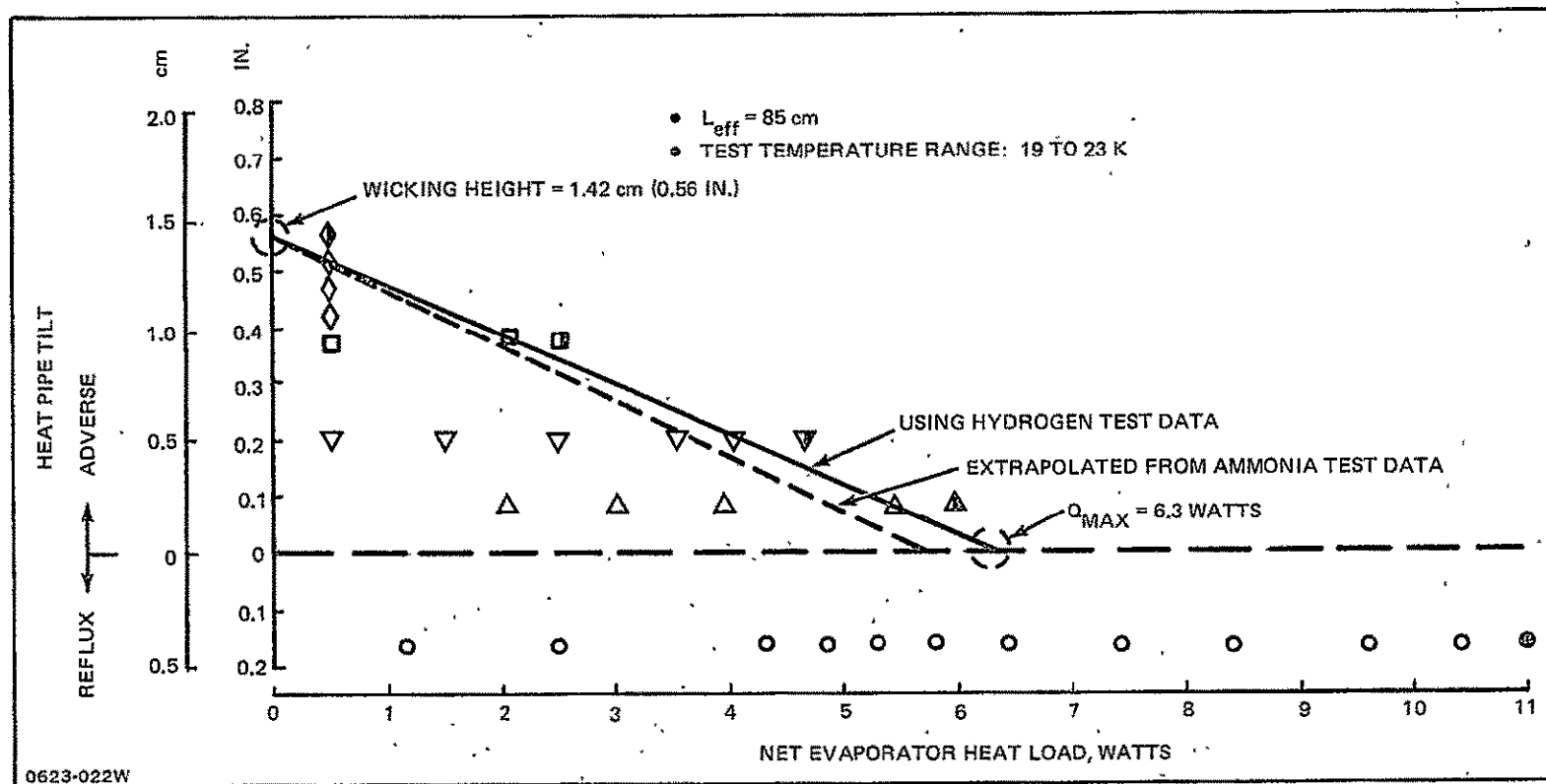


Fig. 22 Hydrogen Heat Pipe Performance Data, Q_{MAX} vs HP Tilt

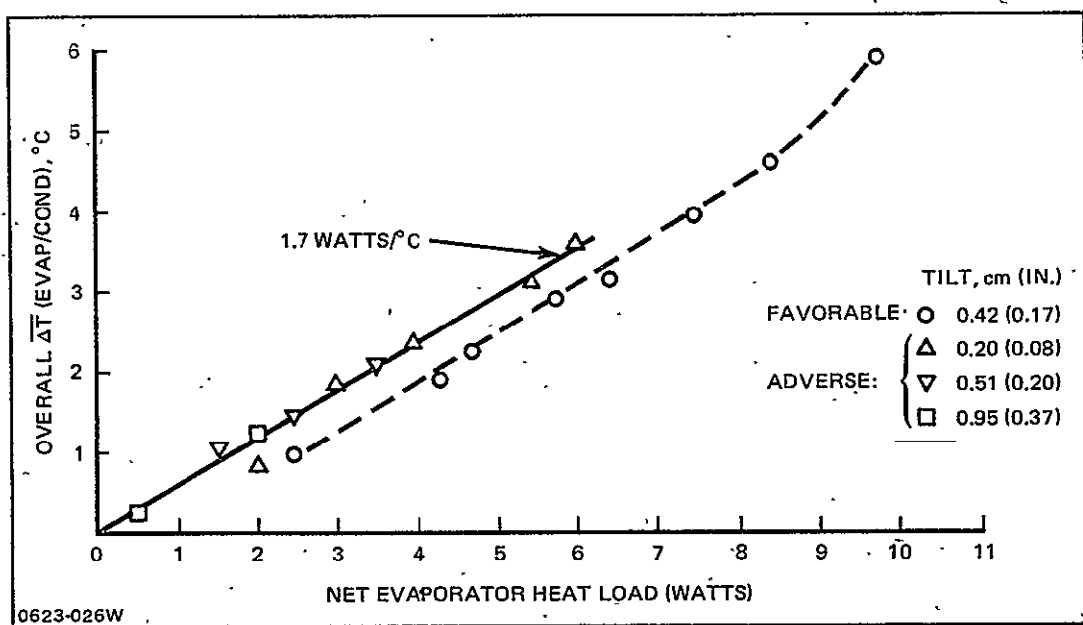


Fig. 23 Hydrogen HP Performance, Overall Temperature Gradient

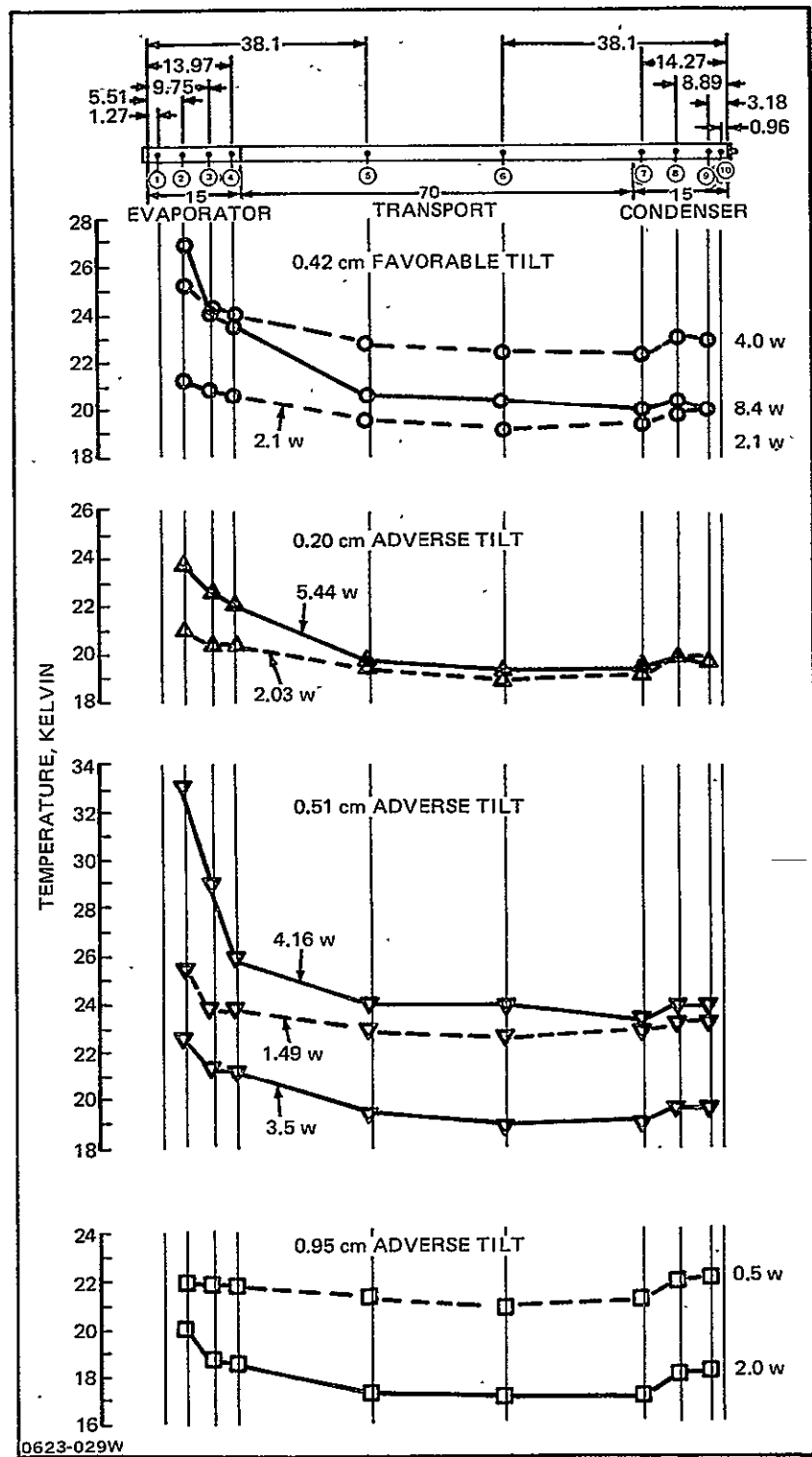


Fig. 24 Hydrogen HP Performance, Temperature Profiles

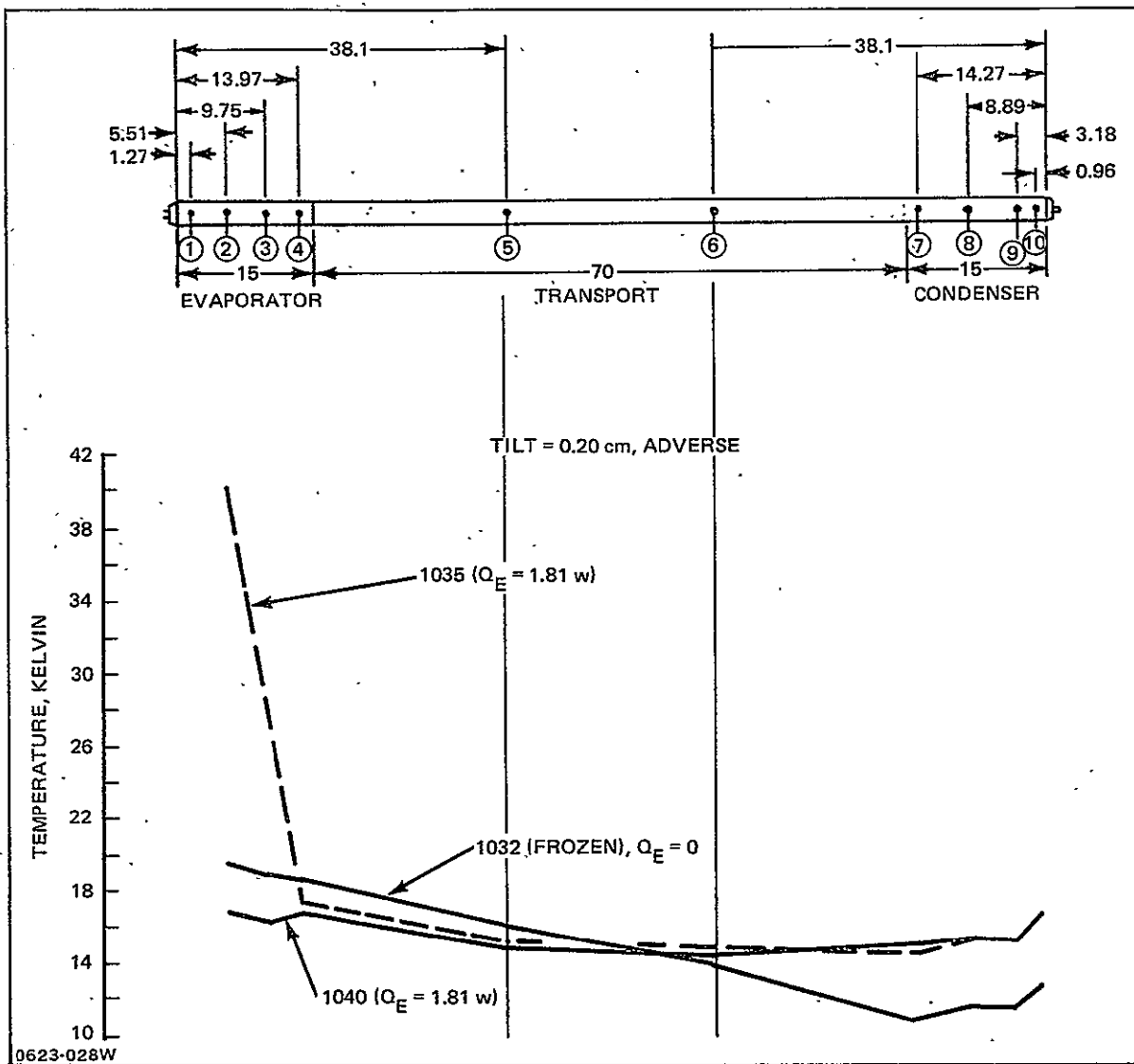


Fig. 25 Heat Pipe Recovery from Frozen Condition

~~PREGEDING PAGE BLANK NOT FILMED~~

Section 8

IMPROVED RE-ENTRANT GROOVE CONFIGURATION

The important shortcomings of the re-entrant groove rounded fin tip profile were the relatively poor film heat transfer coefficients ($h_{evap} = 2014 \text{ w/m}^{20}\text{C}$, $h_{cond} = 5362 \text{ w/m}^{20}\text{C}$ with ammonia). In an effort to overcome these deficiencies, a separately funded in-house development program was initiated. Attempts were made to improve the film coefficients by modifying the groove profile. The most promising of these modifications created a convergent entrance to each groove.

Tests with ammonia on this modified design were very encouraging, as evidenced by the data given in Figure 26. The maximum transport capacity was 104 w-m, while the static wicking height increased markedly to 4.3 cm. More importantly, the primary test objective was achieved, since the evaporator and condenser film coefficients improved greatly, measuring $7900 \text{ W/M}^{20}\text{C}$ and $14,000 \text{ W/M}^{20}\text{C}$, respectively, for an overall conductance of $20.2 \text{ W/}^{\circ}\text{C}$.

These results are significant because the large improvements in static wicking height and film coefficients were realized with only a very small decrease in transport capacity. This was due to a lower net cross sectional flow area per groove. These same modifications, applied to initially larger grooves, could produce high performance, low cost heat pipes with increased wicking height, high film heat transfer coefficients, and significantly greater transport capacity than is provided by currently available axial groove profiles.

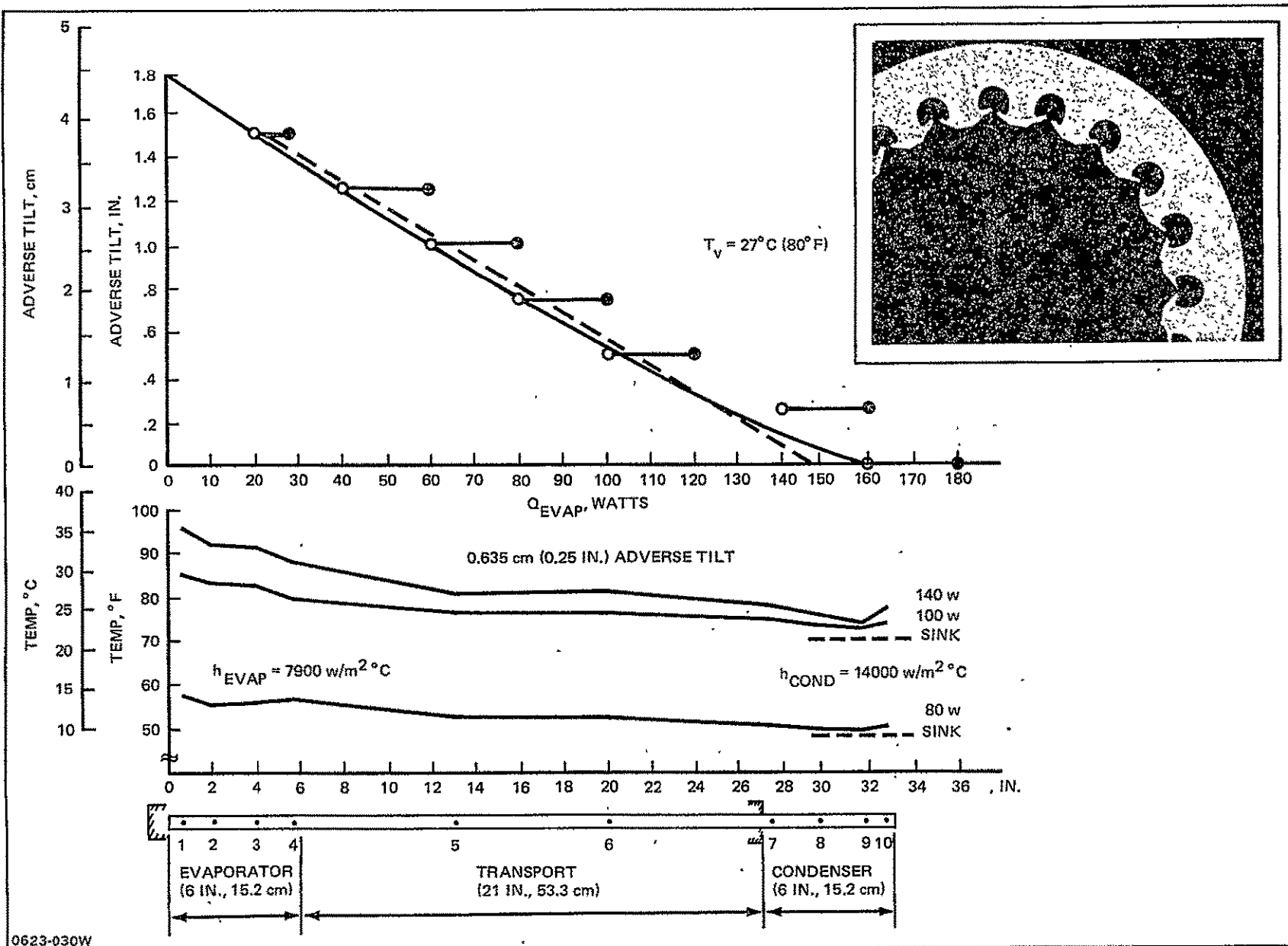


Fig. 26 Improved Re-Entrant Groove HP Performance

~~PREGEDING PAGE BLANK NOT FILMED.~~

Section 9

CONCLUSIONS

- Axial groove heat pipes with re-entrant groove profiles can be produced in useful quantities.
- A slight modification to the groove profile, creating a convergent entrance, after the extrusion process would permit heat pipes to be built that are uniquely suited to cryogenic fluids, especially hydrogen. These heat pipes would provide superior overall thermal performance with a significantly lower fluid inventory, which greatly simplifies storage pressure requirements. This can result in lighter weight heat pipes, due to thinner walls, or a smaller excess vapor reservoir which simplifies packaging.
- Working with hydrogen fluid is not much different than working with other cryogens, such as methane, which can result in high storage pressures. The important considerations are materials (avoiding hydrogen embrittlement), storage pressure containment, and low temperature test requirements. The last item can be expensive if an expendable liquid helium coolant is used.

PRECEDING PAGE BLANK NOT FILMED.

Section 10

REFERENCES

1. Schlitt, K.R., Kirkpatrick, J.P., and Brennan, P.J., "Parametric Performance of Extruded Axial Grooved Heat Pipes From 100 K to 300 K," Progress in Astrodynamics and Aeronautics, Vol. 39, Heat Transfer with Thermal Control Applications, pp. 215-234, MIT Press.
2. Harwell, W., Quadrini, J., Sherman, A., and McIntosh, R., "Cryogenic Heat Pipe Experiment: Flight Performance Onboard a Sounding Rocket," AIAA Paper 75-729, May 1975.
3. Harwell, W., Haslett, R., and Ollendorf, S., "Instrument Canister Thermal Control," AIAA Paper 77-761, June 1977.
4. Harwell, W., Kaufman, W.B., and Tower, L.K., "Re-entrant Groove Heat Pipe," AIAA Paper 77-773, June 1977.
5. NASA SP-3089, Hydrogen Technological Survey - Thermophysical Properties, R. McCarthy.
6. "B-W-R Constants and New Correlations," by H.W. Cooper and J.C. Goldfrank, Hydrocarbon Processing, Vol. 46, No. 12, pp 141 - 146, Dec 1967.
7. B&K Engineering, "Summary Report for Axially Grooved Heat Pipe Study," prepared under NASA-GSFC Contract NA55-22562, June 1977.
8. "Heat Pipe Manufacturing Study," Final Report for Contract NAS5-23156, August 1974.

Appendix A
COMPUTER CODE FOR PARAMETRIC STUDY OF RE-ENTRANT GROOVE GEOMETRIES

FILE KOSSON FORTRAN A

C A L L D A T A

```

C REENTRANT GROOVE DESIGN PROGRAM (REDP) KOS00010
DIMENSION A(4),D(4),CV(4),PV(4),Z(4) KOS00020
G=32.1693*3600.**2 KOS00030
PI= 3.141596 KOS00040
KOS00050
C HYDROGEN VIRIAL COEFFICIENT CONSTANTS FOR TEMP RANGE 100 TO 500 K KOS00060
B1 = 42.464 KOS00070
B2 = -37.1172 KOS00080
B3 = -2.2982 KOS00090
B4 = -3.0484 KCS00100
X11= 109.781 KCS00110
C0 = 1310.5 KOS00120
C1 = 2.1486 KOS00130
X21= 20.615 KOS00140
XMW= 2.01594 KOS00150
C FRICTION COEFFICIENTS KOS00160
A(1)=16. KOS00170
A(2)=.0000331 KOS00180
A(3)=.0791 KOS00190
D(1)=-1. KOS00200
D(2)=.69 KOS00210
D(3)=-.25 KOS00220
Z(3)=1. KOS00230
C DESIGN TEMP = 20 K (-423.6 F) KOS00240
C MAX STORAGE TEMP = 322 K (120 F) KOS00250
C HEAT PIPE LENGTHS ARE INPUT IN CM. KOS00260
C EXTRUSION IS 6063 AL WITH YS = 8250 PSI KOS00270
READ(1,100)TD,TS,YS,XLEV,XLTR,XLC KOS00280
READ(1,100)DO,T,RF,W1,S1,DOMAX,DELT KOS00290
READ(1,101)N,KT,ND,NMIN KOS00300
READ(1,100)EPS,F4,DT KOS00310
C KT = 0, CHANGING ONLY DO KOS00320
C KT= 1, DECREASE N BY ND, KEEP S & T, INCREASE RG KOS00330
C KT =2, DECREASE N BY ND, KEEP S & RG, INCREASE T KOS00340
C KT =3, DECREASE N BY ND, KEEP T & RG, INCREASE S KOS00350
C KT =4, VRES = 0, FIND T & RG FOR GIVEN DC,S, & N KOS00360
K4=0 KOS00370
WRITE(6,102)TD,TS,YS KOS00380
WRITE(6,118)XLEV,XLTR,XLC KOS00390
W=W1/2. KOS00400
XLEVF=XLEV/30.48 KOS00410
XLTRF=XLTR/30.48 KOS00420
XLCF =XLCF/30.48 KOS00430
XLEF=XLEVF/2.+XLCF/2.+XLTRF KOS00440
XLF=XLEVF+XLCF+XLTRF KOS00450
WRITE(6,104)RF,W1,S1 KOS00460
RHOL = PROP(1,13,TD) KOS00470
RHOV = PROP(3,13,TD) KOS00480
XMUL = PROP(2,13,TD) KOS00490
XMUV = PROP(4,13,TD) KOS00500
STEN = PROP(5,13,TD) KOS00510
XLAT = PROP(6,13,TD) KOS00520
PVAP = PROP(8,13,TD) KOS00530
CONDL = PROP(7,13,TD) KOS00540
XNL = G*STEN*XLAT*RHOL/XMUL KCS00550

```

Appendix A (Cont)

FILE KOSSON FORTRAN A	C A L L D A T A
XNV = G*STEN*XLAT*RHOV/XMUV	KOS00560
AGFOM= STEN/RHOL*144.	KOS00570
WRITE(6,108)XMUL,XMUV,STEN,XLAT	KOS00580
S=S1/2.	KOS00590
THETP = PI/N	KOS00600
SNTHP= SIN(THETP)	KOS00610
TSR = TS +459.6	KOS00620
TSK = TSR/1.8	KOS00630
X1 = X11/TSK	KOS00640
X2 = X21/TSK	KCS00650
B=B1*X1**.25+B2*X1**.75+B3*X1**1.25+B4*X1**1.75	KOS00660
BE=B*.0079458	KOS00670
X2TST= 1./X2**3	KOS00680
IF(X2TST.LT.100.)GO TO 202	KOS00690
C= C0*SQRT(X2)*(1.+C1*X2**3.)	KOS00700
GO TO 203	KOS00710
202 C=C0*SQRT(X2)*(1.+C1*X2**3.)*(1.-EXP(1.-1/X2**3.))	KOS00720
203 CE=C*.0079458**2	KOS00730
BP=B	KOS00740
R=8.31432	KOS00750
C R IN J/(MOL-K)	KOS00760
CP=(C-B**2)/R/TSK	KOS00770
300 RO = DD/2.	KOS00780
RG=((RG-T)*SNTHP-S)/(1.+SNTHP)	KOS00790
310 ALPHF=ARSIN((RF+W)/(RF+RG))	KOS00800
S17 = (RF+RG)*COS(ALPHF)	KOS00810
S01 = RO-T-RG	KOS00820
S07 = S01 -S17	KOS00830
SNTHF = (RF+W)/S07	KOS00840
THETF = ARSIN(SNTHF)	KOS00850
IF(THETF.LT.THETP) GO TO 200	KOS00860
WRITE(6,105)THETF,THETP	KOS00870
GO TO 1000	KOS00880
200 S08 = S07/COS(THETF)	KOS00890
PHIF = PI/2.-ALPHF	KCS00900
AN1 =((RF+W)*S17/2.-ALPHF*RG**2/2.-PHIF/2.*RF**2)*2.	KOS00910
BETAF = PI/2.-THETF	KOS00920
RI = S08-RF	KOS00930
AN2= ((RF+W)*S07/2.-THETF/2.*RI**2-EETAF/2.*RF**2)*2.	KOS00940
ALG = PI*RG**2+AN1+AN2/2.-PI/4.*W**2	KOS00950
AL = N*ALG	KCS00960
AV = PI*RI**2+N*(AN2/2.+PI/4.*W**2)	KOS00970
C MAX STORAGE PRESSURE CALCULATION	KOS00980
PS = YS*T/(RO-T)	KOS00990
C PS & PMAX IN PSI	KOS01000
C P IN MEGAPASCALS (PASCAL = N/M**2)	KOS01010
P=PS*.0068948	KOS01020
C SUPERCRITICAL DENSITY CALCULATION FOR STORAGE T AND P	KOS01030
VB= R*TSK/P+BP+CP*P**2	KOS01040
RHT1 = 1./VB	KOS01050
PT1=R*TSK*RHT1*(1.+B*RHT1+C*RHT1**2)*145.04	KOS01060
RHT2=1.01*RHT1	KOS01070
PT2=R*TSK*RHT2*(1.+B*RHT2+C*RHT2**2)*145.04	KCS01080
206 RHTN=(RHT2-RHT1)*(PS-PT2)/(PT2-PT1)+RHT2	KOS01090
PTN=R*TSK*RHTN*(1.+B*RHTN+C*RHTN**2)*145.04	KOS01100

ORIGINAL PAGE IS
OF POOR QUALITY

Appendix A (Cont)

FILE KOSSON FORTRAN A

C A L L D A T A

```

        IF(ABS(PTN-PS).LT.1.)GO TO 207          KOS01110
        PT1=PT2          KOS01120
        PT2=PTN          KOS01130
        RHT1=RHT2          KOS01140
        RHT2=RHTN          KOS01150
        GO TO 206          KOS01160
207   RHOBM=RHTN          KOS01170
        RHOB=RHOBM*125.85          KCS01180
C     RHOB = PCF , RHOBM = MOL/CC          KOS01190
C     CHARGE AND RESERVOIR VOLUME CALCULATIONS PER FOOT OF PIPE LENGTH KOS01200
        ALF = AL/144.          KOS01210
        AVF = AV/144.          KOS01220
        VRES= ((RHOL-RHOB)*ALF+(RHOV-RHOB)*AVF)/(RHOB-RHOV)*1728.          KOS01230
        IF(KT.EQ.4)GO TO 305          KOS01240
C     TRANSPORT CAPACITY CALCULATIONS          KOS01250
        IF(VRES.GT.0.)GO TO 201          KOS01260
205   VRES = 0.          KOS01270
        RHOB= (RHOL*ALF+RHOV*AVF)/(ALF+AVF)          KOS01280
        RHOBM=RHOB*.0079458          KOS01290
        PMAX = R*TSK*RHOBM*(1.+B*RHOBM+C*RHOBM**2)*145.04          KCS01300
201   H = AGFON*(1./W-1./RI)          KOS01310
        DL= 2.*RG/12.          KOS01320
        DV= 2.*RI/12.          KOS01330
        QL=(12./W-12./RI)/32./(1./(XNL*ALF*CL**2.)+1./(XNV*AVF*DV**2.))          KOS01340
C     CHECK FOR TURBULENT VAPOR FLOW          KOS01350
        Q1=QL/XLEF          KOS01360
        RE1=Q1*DVL/(XMUV*XLAT*AVF)          KOS01370
        IF(RE1.LE.2300.)GO TO 208          KOS01380
        CL=32.*STEN*XLEF/(ALF*DL**2*XNL)          KOS01390
        DPC=STEN*(12./W-12./RI)          KOS01400
        REN=RE1          KOS01410
        QN=Q1          KOS01420
        KJ=0          KOS01430
213   DPV=0.          KCS01440
        Z(1)=2300./REN          KOS01450
        Z(2)=3900./REN          KOS01460
        IMAX=2          KOS01470
        IF(Z(2).GT.1.)GO TO 209          KOS01480
        IMAX=3          KOS01490
209   DO 210 I=1,IMAX          KCS01500
        IF(I.GT.1)GO TO 214          KOS01510
        ZI=0.          KOS01520
        GO TO 215          KOS01530
214   ZI=Z(I-1)          KOS01540
215   CV(I)=2.*A(I)*(DV/(XMUV*XLAT*AVF))**D(I)/(G*RHOV*DV*(XLAT*AVF)**2)          KOS01550
        PV(I)=CV(I)*(XLEV*XLCF)*QN**((D(I)+2.)/(3.+D(I))*(Z(I)**(3.+D(I))-KOS01560
        IZI**((3.+D(I))))          KOS01570
210   DPV=DPV+PV(I)          KOS01580
        DPV=DPV+CV(IMAX)*XLTRF*QN**((D(IMAX)+2.))          KOS01590
        DPL=CL*QN          KOS01600
        DPN=DPV+DPL          KOS01610
        DPOP=ABS(DPN-DPC)/DPC          KCS01620
        IF(DPOP.LT..001.)GO TO 211          KOS01630
        IF(KJ.GT.0)GO TO 212          KOS01640
        DP I=DPN          KOS01650

```

Appendix A (Cont)

FILE KOSSON FORTRAN A

C A L L D A T A

```

KJ=1                                KOS 01660
QN=Q1*DPC/DPN                      KOS 01670
REN=RE1*DPC/DPN                      KOS 01680
GO TO 213                            KOS 01690
212 DP2=DPN                           KOS 01700
Q2=QN                               KOS 01710
QN=Q2+(Q1-Q2)*(DPC-DP2)/(DP1-DP2)   KCS 01720
REN=RE1*QN/Q1                        KCS 01730
GO TO 213                            KOS 01740
211 RE=RE1*QN/Q1                      KOS 01750
WRITE(6,117)RE                         KOS 01760
QL=QN*XLEF                           KOS 01770
208 QLWI = QL*12./3.413                KOS 01780
QLWCM=QLWI*2.54                      KOS 01790
XMT = RHOB*(ALF+AVF+VRES/1728.)      KOS 01800
XMGPF = XMT*453.59237                 KOS 01810
DG =2.*RG                             KOS 01820
DI =2.*RI                             KOS 01830
VREST=VRES*XLF                       KOS 01840
XMGT=XMGPF*XLF                       KCS 01850
WRITE(6,103)DG,T,N                   KOS 01860
WRITE(6,106)S,DI,DG,H                 KOS 01870
WRITE(6,107)PS,RHOB,RHOL,RHOV        KOS 01880
WRITE(6,109)VRES,XMGPF,QLWI          KOS 01890
WRITE(6,119)VREST,XMGT,QLWCM         KOS 01900
IF(VRES.GT.0.)GO TO 204               KOS 01910
WRITE(6,110)PMAX                      KOS 01920
204 IF(KT.GT.0)GO TO 301               KOS 01930
IF(DOMAX.LE.0.)GO TO 1000              KOS 01940
IF(DOMAX.LE.D0)GO TO 1000              KOS 01950
IF(DELT.LE.0.)GO TO 1000               KOS 01960
WRITE(6,112)                           KOS 01970
T = T + DELT                          KOS 01980
DO = DO + 2.*DELT                     KOS 01990
GO TO 300                            KOS 02000
301 IF(N.LE.NMIN)GO TO 1000            KOS 02010
N=N-ND                               KOS 02020
THETP=PI/N                            KOS 02030
SNTHP=SIN(THETP)                      KOS 02040
IF(KT.GT.1)GO TO 302                  KOS 02050
WRITE(6,113)                           KOS 02060
GO TO 300                            KOS 02070
302 IF(KT.GT.2)GO TO 303               KOS 02080
WRITE(6,114)                           KOS 02090
S01=(S+RG)/SNTHP                      KOS 02100
T= RD-RG-S01                          KOS 02110
GO TO 310                            KOS 02120
303 IF(KT.GT.3)GO TO 304               KOS 02130
S01=RD-T-RG                           KOS 02140
WRITE(6,115)                           KOS 02150
S=S01*SNTHP-RG                         KOS 02160
GO TO 310                            KOS 02170
305 IF(KT.GT.4)GO TO 306               KOS 02180
IF(ABS(VRES).LT.EPS)GO TO 205         KOS 02190
K4=K4+1                              KDS 02200

```

ORIGINAL PAGE IS
OF POOR QUALITY

Appendix A (Cont)

FILE KOSSON FORTRAN A

C A L L D A T A

```
IF(K4.LE.1)GO TO 401 KOS02210
TN=T+F4#VRES*(T-T1)/(VR1-VRES)
GO TO 402 KOS02220
401 TN=T+DT KOS02230
402 VR1=VRES KOS02240
: T1=T KOS02250
T=TN KOS02260
RG=((RO-T)*SNTHP-S)/(1.+SNTHP) KOS02270
GO TO 310 KOS02280
304 K4=0 KOS02290
WRITE(6,116) KOS02300
GO TO 300 KOS02310
306 WRITE(6,111)KT KOS02320
GO TO 1000 KCS02330
100 FORMAT(7F10.4) KOS02340
101 FORMAT(10I3) KOS02350
102 FORMAT(' OPERATING TEMP = ',F10.4,' F , STORAGE TEMP = ',F10.4,' FKOS02370
1, MAX STRESS = ',F10.4,' PSI ')
103 FORMAT(' OUTSIDE DIA.= ',F10.4,' IN. , WALL THICKNESS = ',F10.4,' KOS02380
1 IN., NO. OF GROOVES = ',I3) KOS02390
104 FORMAT(' FILLET RADIUS = ',F10.4,' IN. , GROOVE WIDTH = ',F10.4,' KOS02410
1 IN. , FIN MINIMUM WIDTH = ',F10.4) KOS02420
105 FORMAT(' INCOMPLETE GROOVE LAND , THETF = ',F10.4,' THETP = ',F10.4,KOS02430
14, ' RADIANS')
106 FORMAT(' MIN. FIN S = ',F10.4,'IN. , I.D. = ',F10.4,'IN. , GROOVE KCS02450
1 DIA. = ',F10.4,'IN. , MAX TILT = ',F10.4,'IN.') KOS02460
107 FORMAT(' STORAGE PRESSURE = ',F10.4,' PSI, MEAN DENSITY = ',F10.4,KOS02470
1 PCF, LIQ DENS = ',F10.4,' PCF, VAPOR DENS = ',F10.4,' PCF') KOS02480
108 FORMAT(' LIQ. VIS. = ',F7.4,' VAP. VIS = ',F7.4,' LBM/FT-HR , SUKOS02490
1RFACE TEN. = ',F10.9,' LBF/FT . LAT. HEAT = ',F8.4,' BTU/LBM') KOS02500
109 FORMAT(' RES VOL = ',F8.4,' CU. IN. PER FT. , WORKING FLUID = ',FKOS02510
110.6.' GRAMS PER FT. , TRAN CAP = ',F10.2,' W-IN') KOS02520
110 FORMAT(' NO RESERVOIR NEEDED ./MAXIMUM PRESSURE = ',F10.2) KOS02530
111 FORMAT(' KT = ',I3) KOS02540
112 FORMAT('/', KT = 0, O.D. & THICKNESS INCREASE, I.D. & RG CONSTANT')KOS02550
113 FORMAT('/', KT = 1, N REDUCED, RG INCREASED, S & T FIXED') KOS02560
114 FORMAT('/', KT = 2, N REDUCED, T INCREASED, S & RG FIXED') KOS02570
115 FORMAT('/', KT = 3, N REDUCED, S INCREASED, I.D. & RG FIXED') KOS02580
116 FORMAT('/', KT = 4, VRES = 0, FIND T & RG FOR DO. S. & N FIXED') KOS02590
117 FORMAT(' VAPOR FLOW NOT LAMINAR, REYNOLDS NO. = ',F10.3) KOS02600
118 FORMAT(' EVAP L = ',F10.4,' CM., TRANS L = ',F10.4,' CM., CGND. L =KOS02610
1 ',F10.4,' CM.') KOS02620
119 FORMAT(' RES VOL = ',F8.4,' CU. IN. (TOTAL), TOTAL CHARGE = ',F1KOS02630
10.6.' GRAMS TOTAL, TRAN CAP = ',F10.2,' W-CM.') KOS02640
1000 RETURN KOS02650
C     DEBUG INIT.SUBCHK KOS02660
END KOS02670
```

Appendix B

SAFE HANDLING AND STORAGE PROCEDURES FOR HYDROGEN HEAT PIPES

With a few basic precautions, under ordinary laboratory circumstances hydrogen heat pipes pose no significant safety hazard. This is largely because of the relatively small amounts of hydrogen involved. The storage vessels used for the research grade purity hydrogen gas are size 6 DOT approved cylinders, which contain about 3 grams of gas at 1585 psia. The charge is taken directly from the supply bottle, and one bottle contains enough hydrogen to charge a single one-meter long heat pipe. The total volume occupied by two supply bottles at STP, which is the amount ordered for this program, is less than 100 liters. OSHA regulation, Vol. 39, No. 125, part II, Subpart H, para. 1910.103, Table H-1, defines this as classification IV, a minor hazard.

These minimum precautions should be followed when working with hydrogen heat pipes:

1. Storage - The charge bottles and charged heat pipes should be stored in well ventilated areas. Valves should be securely capped and valve handles removed if left unattended for extended periods.
2. Transfer and Charging - These operations should be done in a well ventilated, no smoking area. All other possible sources of ignition should also be removed.
CAUTION: Do not energize the ionization gauge on the vacuum station unless hydrogen has been purged from all of the lines. Use gaseous nitrogen to purge all lines and to lower concentration of hydrogen when venting to an exhaust hood.

General Safety Precautions with Hydrogen

(extracted from AEC literature)

Summary

Explosion is the main hazard of hydrogen. In air, gaseous hydrogen forms an explosive mixture in the range of 4.1 to 74.2 percent by volume. The liquid is hazardous because, due to evaporation, the gas is always present. A potentially large hazard exists if liquid hydrogen gets loose from the container.

Some safety rules to be followed in handling hydrogen are:

1. Have good ventilation in the area.
2. Purge equipment with an inert gas before adding hydrogen.

3. Purge equipment with an inert gas after removing hydrogen.
4. Check for concentration with a gas analyzer.
5. Allow no smoking or open flames in the area.
6. Avoid static build-up by the use of conducting floors and shoes.
7. Ground equipment.
8. Use only non-sparking tools.
9. Use only approved electrical equipment.
10. Store cylinders of gas and containers of liquid outdoors. No flammables, oxidizers, or corrosive materials should be stored in the same area.
11. Keep caps on cylinders when not in use.
12. Allow only a minimum of personnel in the area.
13. Prevent spills of liquid hydrogen.

Properties of Gaseous Hydrogen

Under normal conditions hydrogen is a colorless and odorless gas. It is the lightest substance known, having a specific gravity of 0.069 (Air=1). It is non-toxic but does not support life. When mixed in the proper proportions with air, oxygen, or other oxidizers, it forms a highly flammable mixture. In air, the explosive limits for normal hydrogen are 4.1 percent to 74.2 percent by volume. Ignition of hydrogen air mixtures takes place with extremely low energy input; an invisible spark can cause an explosion. The auto-ignition temperature is 1085°F.

Containers

The most common method of packaging hydrogen is in seamless steel cylinders. These must be made and used in accordance with ICC regulations. Those made to ICC specifications have the following information stamped on the neck or shoulder:

1. ICC specification number, followed by the service pressure.
2. Serial number of the user (company filling the cylinder).
3. Inspection stamp and date the cylinder was tested.

Each cylinder is given a hydrostatic test when made, and must be retested once every 5 years. The date of retesting is also stamped on the cylinder. Cylinders must be equipped with a safety device consisting of a frangible metal plug with a fusible metal core. Cylinders must not be refilled except with the consent of the owner of the cylinder.

Hydrogen cylinders should be stored in a well ventilated area away from flammable or corrosive materials. The caps should not be removed except when the cylinders are in use.

not to be an exposure hazard to the plant in the event of the worst possible fire.

PREVENTING AN EXPLOSION

The basic safeguards for preventing a hydrogen explosion are the same as those which apply to all flammable gases, namely, to prevent an explosive concentration and eliminate sources of ignition. Some means of accomplishing these are outlined below.

Preventing An Explosive Concentration

Where relatively small quantities of hydrogen are likely to be present with large quantities of air, precaution should be taken to keep the concentration below the lower explosive limit. Ventilation is the best means of achieving this. The amount of ventilation for any location will depend on many factors and should be worked out by a qualified ventilation engineer.

For some purposes, an essentially pure hydrogen atmosphere must be obtained and maintained within a piece of equipment that was initially filled with air. Air within equipment of this type should first be removed either by vacuum, by purging with an inert gas, by displacing with a fluid, or by a combination of these methods. The equipment is then filled with hydrogen, and a slight positive pressure is maintained to prevent leakage of air into the system.

When emptying, it should be evacuated or purged with an inert gas until tests show that the hydrogen is below the explosive limit. Air should never be used to purge hydrogen from this type of equipment, since such a practice would create an explosion hazard while passing through the entire range of explosive concentrations of hydrogen and air.

Whenever processing equipment requires a continuous flow of hydrogen through it, the escaping hydrogen should be burned to prevent its dissemination into areas where it could cause an explosion hazard. This scheme of burning hydrogen can be applied in a number of different situations, but provision must always be made to insure relighting of the flame if the flow of hydrogen should stop and then start again.

The explosive range of hydrogen can be varied by adding another gas as a diluent. In general, inert gases tend to raise the lower explosive limit, while flammable gases (with an upper limit below that of hydrogen) will lower the upper explosive limit. This method has been used in some instances to reduce the hazard.

Determination of the concentration of hydrogen should not be left to guesswork. Because of entrainment of foreign matter, people sometimes think they can see or smell

hydrogen. This is not a safe method of detection! Instruments for the detection of hydrogen and measurement of its concentration are commercially available. These are of various types, ranging from small portable units to large fixed units which will sample many points continuously.

This instrument can be indicating or recording and can be made to cause automatic actuation of warning devices or other equipment. The manufacturer's instructions should be followed carefully in using these instruments.

Elimination of Sources of Ignition

All sources of ignition should be guarded against:

- a. Open Flames. Smoking, welding, and open flames should not be permitted where hydrogen is present.
- b. Electricity. All electrical equipment should conform to the applicable provisions of the National Electrical Code. Even with the proper equipment, provision should be made to assure that the interior of electrical equipment is not exposed while the circuit is energized or when hydrogen is liable to be present.
- c. Metallic Sparks. Nonferrous tools should be used to avoid sparks. The basic precaution is to permit no work on the system until the area has been tested and found safe.
- d. Static Electricity. Precautions should be taken to avoid the buildup of static electricity. This can be done by grounding equipment and by use of conductive floors and shoes.
- e. Lightning. The installation should be protected from lightning
- f. General Sources. Hydrogen-air mixtures are unusually sensitive, and there have been accidents where the mechanics of ignition are not readily explained. Hydrogen discharging from a cylinder has been known to ignite spontaneously. Because of this phenomenon, the general practice of opening the valve slightly to check for fouling, and to blow dirt out of the fittings on compressed gas cylinders, should not be done with hydrogen.

MINIMIZING THE EFFECTS OF A HYDROGEN EXPLOSION

While the primary safety objective is to prevent a hydrogen explosion, it is necessary to realize that the potential danger is always present. Steps should be taken to minimize injury to people or damage to equipment and buildings, should an explosion occur. Pre-planning must take place in order to keep people as far removed as practicable, and to keep the

number of exposed people to a minimum. Measures can be taken to reduce and limit the effects of an explosion. Among these is venting (covered further below).

Equipment

Apparatus in which hydrogen is used is generally equipped with vents for normal operating requirements, as well as special vents to protect the equipment and personnel in the event of an explosion. Vents of both types should be terminated at a safe location (generally far enough above the building roof so that there is no hazard to personnel or plant if the gas ignites). Care should be taken in arranging vents so that there are no higher parts of the equipment in which hydrogen can be entrapped. While there are no approved flame arrestors for hydrogen use, protection can be obtained through liquid seals or packed column vents. Because hydrogen will pick up moisture, when using a liquid-seal flame arrestor, it is necessary to insulate all outside vent piping to prevent freezing.

Closed vessels operated under pressure should be equipped with safety devices to relieve any excessive pressure. There is a pressure rise during an explosion even with open, unobstructed vents. Any delay in the opening of venting devices tends to increase the force of the explosion. It is essential that pressure relief devices start to open at pressures as low as tolerable. Also, the construction must be light so that full opening can be quickly attained. Vent pipes should be of a straight run and as short as safely possible.

For closed vessels, the maximum explosion pressure reached will be influenced by the initial pressure, the bursting strength of the rupture disk, the ratio of the vent area to the volume of the vessel, and by the physical dimensions of the vessel. In pipelines or long narrow tanks, it may not be possible to have any effective venting. When the ratio of length to diameter is greater than 60, it appears that a detonation can occur. This will quickly build up pressures on the order of thousands of pounds per square inch, even though one end of the container is open to the atmosphere. In closed vessels, the critical ratio will be reduced as the initial pressure is increased. However, at ratios less than critical, a high length to diameter ratio is advantageous due to the effect of the wall cooling, and the maximum explosion pressure is reduced.

Buildings

Buildings in which any significant hydrogen explosion can occur should be provided with special explosion vents as well as normal venting. Explosion vents can take many forms — windows, doors, panels, walls, even the roof. Care must be taken in venting the blast to see that it is channeled to an area where people or equipment will not be harmed. Venting devices must be maintained to insure that they will operate properly when needed.

FIGHTING FIRES

The only effective way to fight a hydrogen fire is to shut off the flow of gas. If it is necessary to extinguish the flame in order to reach a place where the hydrogen flow can be shut off, a dry chemical extinguisher is recommended.

Dry chemical is no more effective than CO₂, but it provides greater shielding of the extinguisher operator, longer range, and visibility of the flame.

However, if the fire is extinguished without stopping the flow of gas, an explosive mixture may form, creating a more serious hazard than the fire itself. The usual attack would be to prevent the fire from spreading, and to let it burn until the hydrogen is consumed. The plant or local fire department should be kept up to date on hydrogen installations (as well as other hazardous areas) so that they can make plans to meet any emergency.

Appendix C

SAFE HANDLING AND STORAGE OF LIQUID HELIUM

The following procedures for the safe storage, transfer, and handling of liquid helium have been mostly extracted from LINDE literature. As stated here, they are only applicable to laboratory-scale test situations using a maximum quantity of 500 liters at any one time.

Summary of Procedures for Hydrogen Heat Pipe Test Set-Up

Storage. The liquid helium storage container (LINDE LSHe-500) should be stored in a well ventilated area. Delivery from the supplier should be scheduled to coincide with the actual need. The daily boil off rate is about 1% per day, which makes long storage periods wasteful.

LHe Withdrawal and Transfer

1. The entire system must be properly pre-cooled and pre-conditioned before admitting liquid helium. All transfer lines, including the thermal vacuum chamber feed thru, must be vacuum jacketed and designed for helium use. Using separate transfer lines for each step, the following preconditioning sequence is recommended:
 - a) pre-cool system with liquid nitrogen
 - b) purge system with gaseous helium to remove nitrogen and air
 - c) connect to LHe supply while admitting saturated helium vapor
2. To tap the LHe bottle follow these steps:
 - a) Use two (2) men wearing protective equipment (face mask, insulated gloves)
 - b) Open valve at top of dip tube and remove protective cap and collar
 - c) Slowly crack liquid withdrawal valve until wide open (lever in vertical position)
 - d) Slowly insert the dip tube until it seats, being careful to keep it vertical at all times. Vapor will start to escape thru dip tube.
 - e) Close dip tube valve. **CAUTION:** Never attempt to close the liquid withdrawal valve on the LHe bottle when the dip tube is inserted. It will be crushed.
 - f) Connect vacuum jacketed transfer line to dip tube
 - g) Open dip tube valve letting saturated helium vapor escape. Disconnect gaseous

helium purge line from T/V chamber feed thru, and connect the LHe transfer line making sure that vapor is always present.

- h) Hand tighten connections

Helium Gas Pressurization of the LHe Bottle

To permit LHe withdrawal at higher flow rates than available with natural internal boil off, the vapor space must be pressurized with gaseous helium. An overpressure of about 2-3 psig is applied through the gas phase valve and provides continuous delivery of about 5 liters/min. Note that only about 75 liters per 500 can be withdrawn with natural boil off pressure alone. The procedure is as follows:

1. Keeping a constant flow of helium gas, make loose connection to gas relief valve.
Shut helium gas.
2. Crack open relief valve and purge loose connection from LHe bottle side. Tighten connection as vapor is expelled. Close gas relief valve.
3. Set gas helium pressure above LHe bottle pressure.
4. Open gas relief valve on LHe bottle.
5. Use pressure regulator on gas helium bottle to adjust flow rate.

Treatment of Cold Helium Vapor

The helium vapor is extremely cold (20 K) as it exits the vacuum chamber. It must be heated to above 100 K or else it will freeze the air upon contact, producing a hazardous situation. After heating the helium vapor above 100 K, it should be exhausted directly to the outside atmosphere (or to a ventilating system which connects to the outside). This outside vent should be hooded and well isolated from potential human contact.

General Laboratory Procedures (Extracted from LINDE literature)

Specific properties of helium are given in Table C-1.

Storage and Transfer of Liquid Helium

In most instances, the use point of liquid helium is an appreciable distance from the liquefier. This factor, coupled with the sizable loss of liquid helium that occurs in transfers, has resulted in the combination of the transport and storage functions into a single item of equipment (vacuum insulated supply bottles).

Liquid can be stored in the supply vessels until needed, but the access paths to both the liquid and overlying gas spaces of the vessels must remain closed, and their connections must be tightly capped. During storage, the relief valve will control container pressure, releasing small amounts of gas corresponding to the normal evaporation rate of the container.

Table C-1 Specific Properties of Helium.

MOLECULAR SYMBOL	He	
MOLECULAR WEIGHT	4.0026	
FREEZING POINT (1 atm)	*	
BOILING POINT (1 atm)	7.59° R (-452.08° F)	4.21° K (-268.94° C)
LIQUID DENSITY AT nbp	7.798 lb/ft ³ 0.2754 lb/liter	0.125 gm/cm ³ 124.9 gm/liter
GAS DENSITY AT nbp	1.04 lb/ft ³ 0.0368 lb/liter	0.0167 gm/cm ³ 16.7 gm/liter
GAS DENSITY AT NTP**	0.01034 lb/ft ³	0.1656 gm/liter
GAS DENSITY AT STP***	0.01114 lb/ft ³	0.1784 gm/liter
HEAT OF VAPORIZATION AT nbp (LATENT HEAT)	8.72 Btu/lb 2.40 Btu/liter	20.3 joules/gm 605 cal/liter 0.704 watt-hr/liter
C _p OF LIQUID AT nbp	1.08 Btu/lb-°R	4.48 joules/gm-K
C _p OF GAS AT STP***	1.248 Btu/LB-°R	5.222 joules/gm-K
C _p /C _v AT STP***	1.66	1.66
SUPERHEAT EQUAL TO LATENT HEAT	7.0° R	3.9°K
CRITICAL TEMPERATURE	9.4° R (-450.3° F)	5.2° K (-267.9° C)
CRITICAL PRESSURE	33.2 psia	2.26 atm
THERMAL CONDUCTIVITY OF GAS AT NTP**	0.086 Btu/hr, ft ² , °R/ft	1.5 milliwatts/cm ² , K/cm
THERMAL CONDUCTIVITY OF GAS AT STP***	0.082 Btu/hr, ft ² , °R/ft	1.4 milliwatts/cm ² , K/cm
VISCOSITY OF LIQUID AT nbp	75 × 10 ⁻⁹ lb-sec/ft ²	36 micropoise
VISCOSITY OF GAS AT STP***	391 × 10 ⁻⁹ lb-sec/ft ²	187 micropoise
VOLUME EXPANSION, LIQUID AT nbp TO GAS AT NTP**	754.2 TO 1	754.2 TO 1
VOLUME EXPANSION, LIQUID AT nbp TO GAS AT STP***	700.1 TO 1	700.1 TO 1
COLOR	NONE	
ODOR	NONE	
TASTE	NONE	

*HELIUM WILL NOT SOLIDIFY AT 1 atm. THE PRESSURE REQUIRED FOR SOLIDIFICATION AT ABSOLUTE ZERO IS CALCULATED TO BE 25 atm. THE APPROXIMATE PRESSURE REQUIRED FOR SOLIDIFICATION AT 4.2° K HAS BEEN DETERMINED EXPERIMENTALLY AS 140 atm.

**NTP = 1 atm (14.696 psia) AT 70° F

***STP = 1 atm (14.696 psia) AT 0° C

CONVERSION VALUES

1 liter	= 0.264172 gal	= 0.035314 ft ³
1 ft ³	= 28.3168 liters	= 7.48052 gal
1 gal (US)	= 3.78541 liters	= 0.133681 ft ³

0623-027W

Small containers of 500 liters or less are designed to provide the user with a great deal of flexibility in removing the product from the container. A major feature is the neck-tube type of access, which permits a wide variety of transfer lines to be inserted. These lines are always vacuum jacketed and are usually 1/2 inch or 3/8 inch outside diameter. Such lines must be designed to provide efficient insulation while liquid is flowing from the container, and also to prevent excessive heat flow through their metal paths to the liquid helium in the container.

Transfer provides a much sterner challenge to efficient handling of liquid helium than storage. This is due to the heat input experienced at the interfaces of the connecting conduit with the storage and receiving apparatus; and in the conduit and valves. Cooldown of the transfer elements and the receiving apparatus also contributes to significant losses, even when pre-cooled with liquid nitrogen. When making such transfers, the evolution of a large amount of helium vapor requires flow passages and relief devices of adequate size. This prevents overpressurizing the apparatus.

Pre-cooling and Purging

Proper cooldown and purge of liquid helium equipment is essential to efficient and safe service.

Some principles to keep in mind in the pre-cool and purge operations are:

1. The use of liquid nitrogen will greatly reduce the liquid helium cool-down loss, but the liquid nitrogen must be completely removed and followed by a helium gas purge. If not removed, either liquid or gaseous nitrogen will freeze at helium temperature, with consequent operational problems and safety hazard due to plugged lines. NEVER use liquid nitrogen to pre-cool a flexible helium transfer line, since it is difficult to remove from the convolutions.
2. Saturated nitrogen vapor at 78 K (- 320^oF) may in some cases prove to be a good alternate cooldown medium, since it avoids the need for liquid nitrogen removal. This may be applicable in equipment where gaseous helium can be used to purge the gaseous nitrogen, but where it would be impossible to remove all the liquid nitrogen.
3. In some cases, particularly where a gaseous helium recirculation system is available, it may be advantageous to pre-cool by using helium gas cooled to 78 K by liquid nitrogen in a heat exchanger. This limits the purge operation to one initial step, and avoids any warmup which might occur when a gaseous helium purge follows a nitrogen cooldown operation.

4. A trace system employing liquid nitrogen or cold gaseous nitrogen might be used to advantage, especially where intermittent transfers are required. The nitrogen should be removed, and the trace system should be purged with gaseous helium prior to liquid helium transfer.
5. Saturated helium vapor has a large amount of sensible heat refrigeration potential, and where possible, the equipment design should permit use of this refrigeration. Final cooldown of transfer lines (even when pre-cooled) should always be accomplished, where possible, by trickling liquid helium into the line immediately prior to transfer, thereby making maximum use of the superheat of the cold vapor to cool the line. Any attempt to cool the line with large quantities of the liquid helium will result in abnormally high evaporation loss from cooldown.
6. Before filling, final purging of a vessel must be performed with pure, dry, helium gas. A minimum of two "volumes" of helium should be bled into the top of the vessel while the contaminated gas is exhausted from the bottom. The term "volume" means the quantity of vessel-temperature gas required to fill the vessel. Thus, a minimum of two liters of ambient temperature gas would be used to purge each liter volume of an ambient temperature vessel, and a minimum of eight liters of ambient temperature gas would be required to purge each liter volume just after nitrogen pre-cooling. The purge helium should be admitted at a slow rate to the top of the vessel, and the discharge removed from the bottom of the vessel.
7. Transfer lines must also be purged before filling or withdrawal. If helium remains under pressure in the vessel to be filled, helium may be bled from the vessel through the transfer line to effect purging. Also, the transfer line can be purged at the same time as the vessel during the final helium purge prior to filling.
8. All nitrogen and helium gas used in the purging and pre-cool operations should be pure and dry.

Withdrawal of Liquid Helium

Because of its very low latent heat of vaporization, liquid helium must always be transferred through well-insulated, vacuum-jacketed lines. Non-vacuum insulation or poor vacuum in vacuum-jacketed lines will result in total loss of liquid.

The following general procedures should be used when withdrawing liquid helium from a helium container. (Adequate pre-cooling and purging described above will not be repeated in detail below, even though some of the final pre-cool and purging operations may occur simultaneously with transfer of helium from supply vessel).

1. Prepare equipment for transfer by proper arrangement of supply and receiving vessels, and interconnecting vacuum-insulated transfer lines. Suitable means for monitoring the helium content of both containers should be provided when desirable.
2. When a withdrawal tube is to be inserted into the supply vessel, place the dip tube at the cooldown position shown in Figure C-1 for several minutes, while letting a small flow of cold helium vapor pass through the line for final pre-cool and purge. An adequate seal should be made between the transfer tube and the supply vessel to prevent atmospheric gases, moisture, and condensed air from entering the container. The seal is also needed to provide for pressure transfer of the liquid helium. Prior to transfer, the dip tube is lowered to the liquid withdrawal position shown in Figure C-1.
3. The transfer component should also be inserted into the receiving vessel, using appropriate techniques for pre-cool and purge requirements.
4. Begin the liquid helium transfer using a low transfer rate, so that much of the final line cooldown can be accomplished using the large refrigeration effect of the cold helium vapor, which results from liquid helium vaporizing within the transfer components.
5. Small quantities of liquid can be transferred using the initial container pressure, plus that which results from insertion of the dip tube. To withdraw larger quantities, pressurize the container through a gas-phase connection with clean, dry, pure, regulated helium gas. External pressurization should be used only when necessary, since introduction of warm gas will vaporize some of the liquid helium in the container. Usual transfer pressures are 1 to 4 psig, depending on the system requirements.
6. If a vacuum-insulated valve and dip tube assembly is used, close the valve at the conclusion of transfer. Promptly remove the connecting hose from the receiving vessel, and then from the valve. Immediately cap the valve and immediately cap the valve outlet. If additional transfers are to be made on the same day, the valve and dip tube assembly can remain in the container. Where possible, transfers should be made in rapid succession to avoid repeating the line cooldown loss.

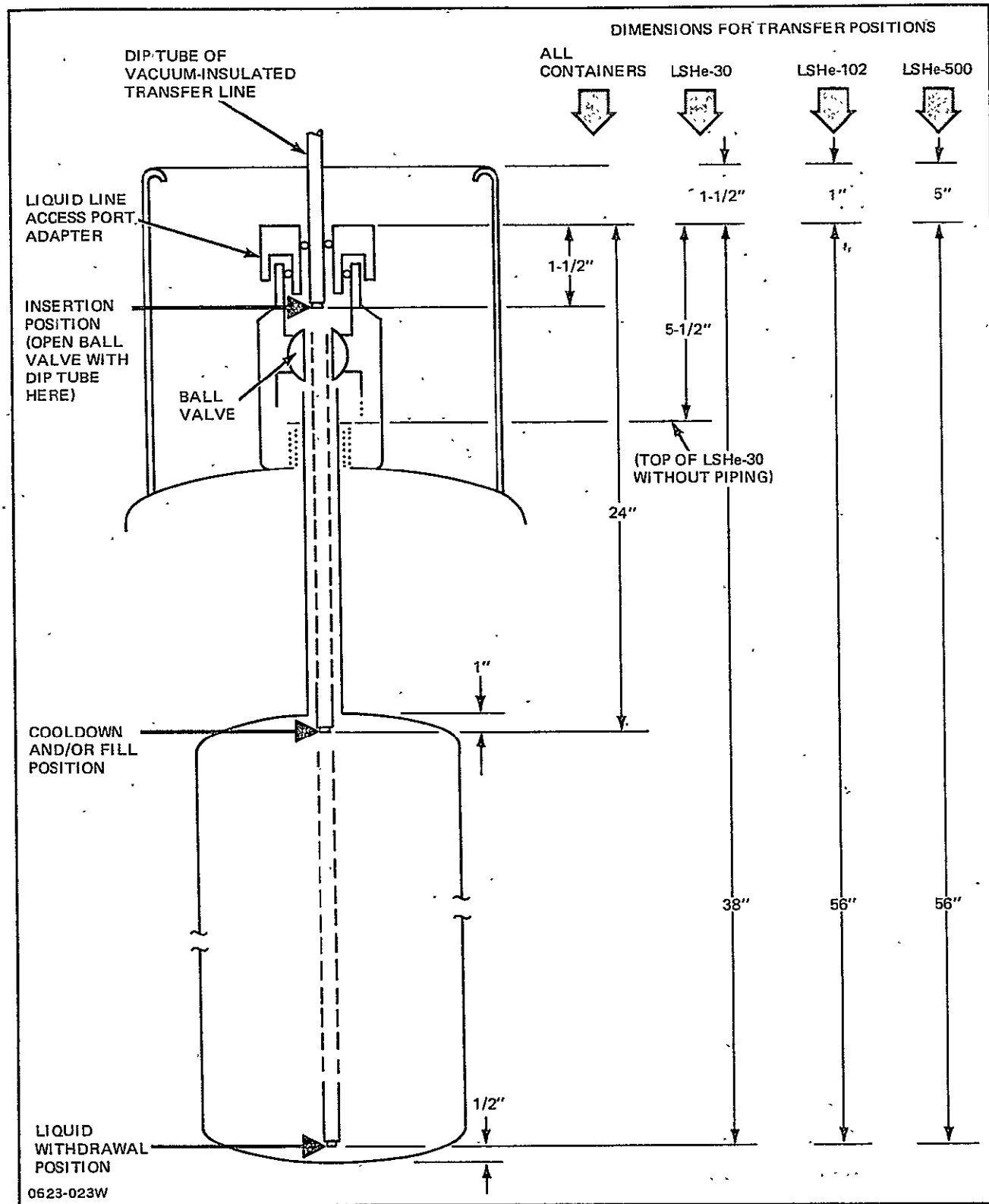


Fig. C-1 Insertion of Transfer Line Into Liquid Helium Container

7. Store the transfer hardware in a suitable location, and protect against internal moisture condensation and contamination.
8. A positive pressure should be maintained in the supplying and receiving vessels to prevent freeze-ups due to air or moisture.

Generally speaking, liquid helium transfers should be made in a reasonably short time period, measured in minutes. Continuous transfers over a few hours should be avoided. The conventional transfer hoses, valves, and bayonets are well suited for short-term transfers, and have been designed for ruggedness and good adaptability. When liquid helium must be transferred over a long period, or repeatedly transferred wherein the components warm up between transfers, design of special components should be considered.

Liquid helium should not be impinged on the mass to be cooled. It should be directed towards the bottom of the vessel to prevent excessive boiling and splashing, and to promote as much final cooling as possible by the cold helium flashoff.



0623-79